macromol

MDPI

Review

Polyphenol–Macromolecule Interactions by Isothermal Titration Calorimetry

Maarit Karonen

Natural Chemistry Research Group, University of Turku, FI-20014 Turku, Finland; maarit.karonen@utu.fi

Abstract: Isothermal titration calorimetry (ITC) is a widely used and valuable technique for studying the binding interactions and the formation and dissociation of molecular complexes. ITC directly measures the energetics associated with the interactions and allows for a precise and complete thermodynamic description of association and binding processes, thereby providing an understanding of the interaction mechanisms. In this review, the role, practical aspects related to the experimental design and setup, advantages, and challenges of using ITC to evaluate polyphenol–macromolecule binding are discussed in detail. The focus is on the possibilities offered by ITC, but at the same time, its limitations are taken into account, especially in the study of complex biological processes and in the subsequent reliable determination of thermodynamic parameters. Polyphenols and proteins typically exhibit exothermic interactions, producing strong signals and distinctive titration curves that can be fitted by one- or two-site binding models; of course, there are exceptions to this. Tannins and tannin fractions usually have a high binding stoichiometry and stronger interactions with proteins than the smaller polyphenols. The driving forces behind these interactions vary, but in many cases, both hydrogen bonding and hydrophobic interactions have been reported. The interactions between polyphenols and polysaccharides or lipid bilayers have been far less studied by ITC in comparison to polyphenol–protein interactions. ITC could be utilized more extensively to study polyphenol–macromolecule interactions, as it is an excellent tool for evaluating the thermodynamic parameters of these interactions, and when used together with other techniques, ITC can also help understand how these interactions affect bioavailability, food applications, and other uses of polyphenols.

Keywords: association; binding; calorimetry; flavonoid; lipid; molecular flexibility; molecular size; polysaccharide; protein; tannin; thermodynamic profile

Academic Editor: Ana María Díez-Pascual

Received: 6 September 2024
Revised: 11 December 2024
Accepted: 6 January 2025
Published: 12 January 2025

Citation: Karonen, M. Polyphenol–Macromolecule Interactions by Isothermal Titration Calorimetry. *Macromol* **2025**, *5*, 2. https://doi.org/10.3390/macromol5010002

1. Introduction

Polyphenols are an interesting group of plant specialized metabolites, also known as secondary metabolites, whose interactions with various biological macromolecules have been studied for decades. They can be classified into flavonoids, stilbenes, lignans, and tannins including three families of compounds: phlorotannins, proanthocyanidins (PAs, syn. condensed tannins), and hydrolysable tannins (HTs), which can be further divided into simple gallic acid derivatives, gallotannins and ellagitannins (ETs); example structures of which are presented in Figure 1. Polyphenols originate from the shikimate-derived phenylpropanoid and/or polyketide pathways, featuring more than one phenolic ring and no nitrogen-based functional groups in their structures and having promising bioactivities and positive health benefits [1]. Polyphenols can have interactions with macromolecules of all kinds, such as well-known associations with proteins [2], carbohydrates [3–6], lipids [7–10],

and nucleic acids [11]. In living plants, polyphenols and macromolecules are compartmentally separated. However, during the processing of plant material, such as in food and beverage preparation, cell structures break down due to shearing and thermal forces. This breakdown allows intracellular contents to mix and interact more freely [6]. These interactions can be complex involving different phenomena, such as adsorption, oxidation, solubilization, and migration [3,6].

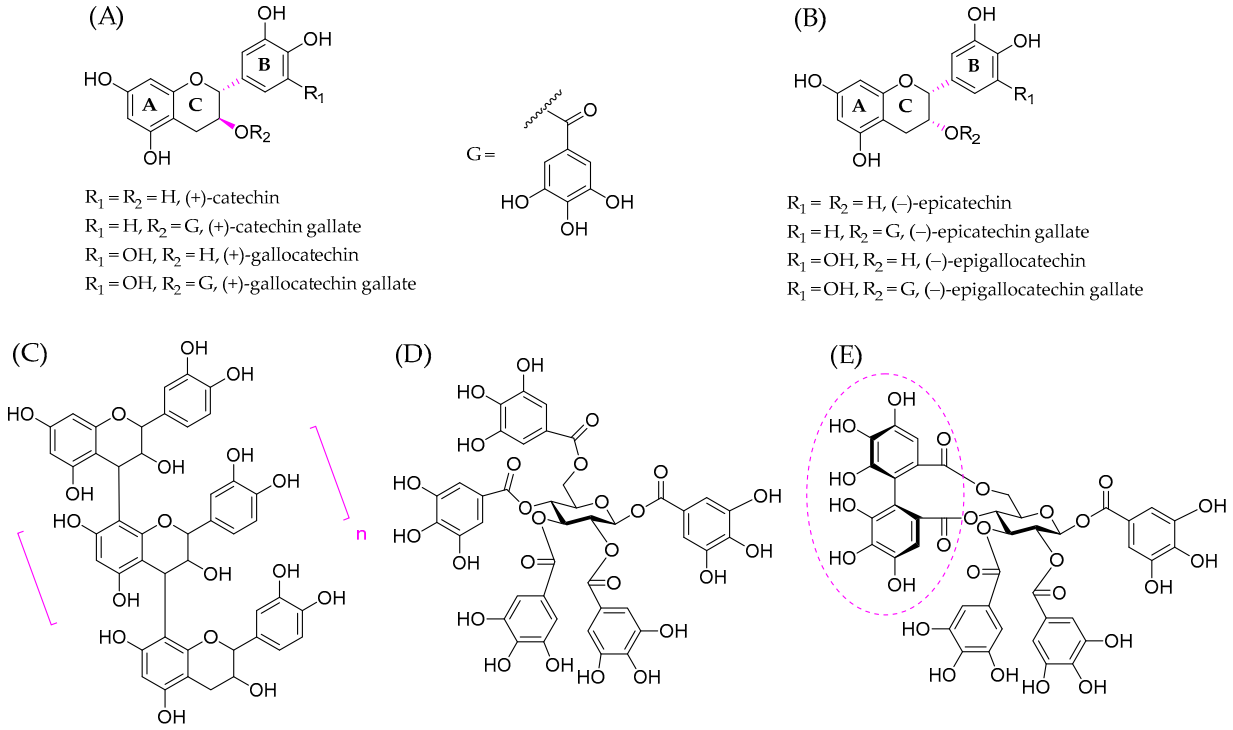

Figure 1. Examples of polyphenols widely studied for their interactions with biological macromolecules: (**A**) flavan-3-ols with *2R,3S* stereochemistry, (**B**) flavan-3-ols with *2R,3R* stereochemistry, (**C**) a B-type procyanidin linked by C4–C8 bonds having the degree of polymerization of $n + 2$, (**D**) pentagalloylglucose and (**E**) tellimagrandin II with the highlighting of the characteristic hexahydroxydiphenoyl group for ellagitannins.

There are various methods to study the interactions between polyphenols and biological macromolecules [2,3]. For example, non-covalent associations between polyphenols and proteins have been studied by using (i) direct methods in dilute solutions, for instance, by isothermal titration calorimetry (ITC), equilibrium dialysis, size exclusion or affinity chromatography, nuclear magnetic resonance spectroscopy, mass spectrometry, and small angle scattering techniques for X-ray and neutrons; (ii) precipitation methods, such as protein precipitation, competitive binding assay, turbidimetry, nephelometry or dynamic light scattering; (iii) indirect study of the consequences of the interaction on the enzyme activity as earlier reviewed by Le Bourvellec and Renard [3]. Of these techniques, ITC is particularly interesting, as it is direct and quantitative, elucidates the thermodynamic profile of the interaction and can also reveal structural relationships. Generally, ITC is a widely used technique in different areas of research for studying intermolecular interactions, primarily for interactions between small molecules and biological macromolecules, such as protein–ligand or metal–ligand interactions [12–14], partition to membranes or polymer surfactant interactions [15], but recently also for binding interactions between synthetic polymers and small molecules, ions, or nanoparticles [16]. It can examine the thermodynamics of polyphenol–macromolecule interactions, providing insights into binding processes and affinities (binding constant K_a), stoichiometry, or the number of binding sides

(n), and thermodynamic parameters, such as enthalpy changes (ΔH), binding entropies (ΔS), and the Gibbs free energy of association (ΔG). If the measurements are performed in different temperatures, the change in the heat capacity of the binding process (ΔC_p) can also be calculated [15,17]. As all biomolecular interactions include changes in heat energies, ITC can offer a comprehensive thermodynamic profile of an interaction process with benefits including reduced sample amounts and the absence of chemical modification or labeling requirements. In addition, it tolerates possible precipitation happening during the interactions and does not limit the size of the interacting species [18]. At its best, it can produce information about the nature of the driving forces responsible for the binding.

2. Practical Aspects Related to ITC

In general, the principle of ITC is simple: the ligand/polyphenol solution is titrated stepwise into the sample cell, which is filled with the macromolecule solution, the heat change caused by each injection is quantified, and after the titration, the heat evolution is analyzed and data fitted allowing the determination of thermodynamic parameters. However, the ITC measurements need to be carefully designed in order to minimize the errors due to incorrect instrument use or conditions, insufficient operator training or instrument calibration [15,19]. On the whole, an ITC experiment can be divided into different steps including planning, preparation of the solutions needed, collection of the raw ITC data together with proper blanks, cleaning of the instrument, correction of the raw ITC data, and final data fitting and analysis. A typical instrumental design consists of a calorimeter controlled by a computer (Figure 2A). Traditional instruments were operated manually, but nowadays the operation can be fully automated, allowing the use of 96-well plates for sample presentation [20,21]. The operating temperatures can vary between 2 and 80 °C, but most often 25 °C (room temperature) and 37 °C (human body temperature) are used. The size of sample cell varies; for example, it can be coin-shaped, made from Hastelloy, with a volume of 200 µL [20], or it can be cylindrical, constructed of gold or Hastelloy, with a standard volume of 1.0 mL [21].

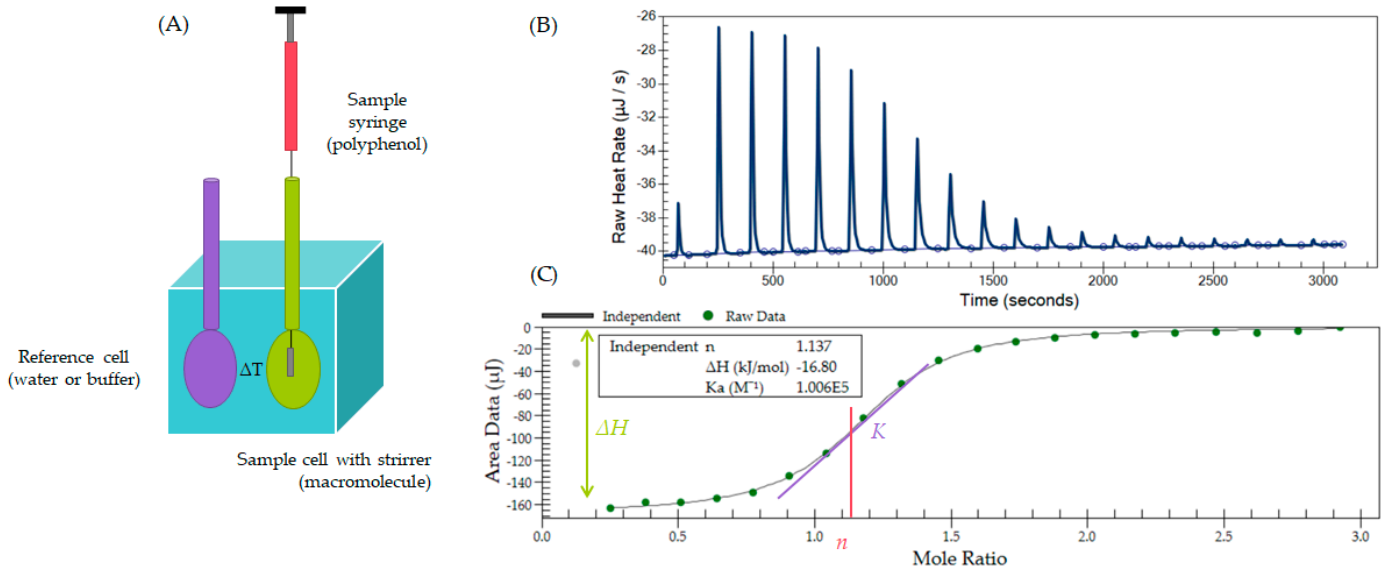

Figure 2. (**A**) Schematic diagram for an isothermal titration calorimeter, (**B**) a model thermogram with exothermic interactions up, and (**C**) a model binding isotherm having sigmoidal shape fitted with one-site model where *Ka* = binding constant, n = number of binding sides, and ΔH = enthalpy change.

The raw data in ITC is the heater power used to maintain the temperature difference between the sample and reference cells at zero ($\mu cals^{-1}$ or μJs^{-1}) [12]. It is obtained as

a thermogram (Figure 2B), i.e., the experimental profile of injections or the plot of heat against the injection number, and then transformed into a binding isotherm (Figure 2C), i.e., the plot of integral heat changes as a function of molar ratio, by the instrumental software. The shape of the binding curve depends on the unitless parameter *c* [22,23]:

$$c = Ka \times [\mathrm{M}] \times n, \quad (1)$$

where [M] is the total concentration of the macromolecule in the sample cell. If the binding is very tight, the *c* value is high, whereas if the binding is weak, the *c* value is low. To obtain a well-defined ITC plot, which allows the determination of thermodynamic parameters, the *c* value should be between 1 and 1000 [23]. Recently, Biswas and Tsodikov [24] suggested that a *c* value between 5 and 20 is optimal for ITC titration, while Brocker et al. [25] recommended around 40 for state-of-the-art microcalorimeters. Additionally, the concentration of the ligand should be ten to fifty times higher than the concentration of the binding sites in the sample cell. Ideally, by the end of the analysis, all binding sites in the sample cell should be saturated (Figure 2B). Although this cannot always be achieved, and experimental compromises may be necessary, the importance of careful planning and testing cannot be overstated.

2.1. Careful Experimental Design and Setup

ITC is a valuable tool for studying the thermodynamics of polyphenol interactions, providing insights that are difficult to obtain with other techniques. However, successful ITC experiments require careful design; this is partly due to the nature of the method as discussed above, but also due to the complexity of the model substances used. In addition, ITC results are sensitive to experimental conditions used, such as temperature, pH, and ionic strength [15]. Small changes in these conditions can significantly affect the binding interactions studied. Typically, ITC measurements are performed in aqueous buffered solutions with exactly the same buffer composition in both the titration syringe and the sample cell [16]. The most common buffers for studying polyphenol–protein interactions include citrate buffer [26–29], phosphate buffer [26] or ammonium acetate buffer [30,31], whereas for membrane studies, phosphate-buffered saline (PBS) [32] or sodium phosphate buffer [7] have been used. Citrate/phosphate buffer is common for polysaccharide interactions [33]. In all cases, the stability of both the polyphenol and the macromolecule in the buffer used must be carefully studied. For example, when the stability of HTs was monitored by UPLC-DAD-MS in a 20 mM sodium phosphate buffer (pH 7), it was noticed that pentagalloylglucose and tellimagrandin II remained stable, retaining 92% and 90% of their initial concentrations after 10 h of incubation, respectively. However, vescalagin dissociated so that only 40% was left [7]. Similarly, it has been noticed that substantial degradation of HTs can happen in PBS [34] and other buffer solutions, especially with long incubation times and pH > 6 [35]. If the stability of polyphenols in the buffer is not known, then a safe approach is to dissolve the samples in the buffer solutions just before each titration.

The role of various parameters, such as the number of injections, injection volume, and delay between injections, as well as the practical parameters like reference power and stirring speed, has been thoroughly reviewed by Bastos and Velazquez-Campoy [15]. They also advise that if there is no prior information about the concentrations or injection volumes to be used, a good starting point is with the titrant concentration in the syringe, i.e., the polyphenol, that is 10–20 times higher than the titrant concentration in the sample cell, i.e., the macromolecule; for example, 200–400 μM in the syringe and 20 μM in the cell [15]. Before the actual ITC measurement, all samples are degassed. The titration syringe and sample cell need to be carefully filled to avoid introducing air bubbles into the system. In

order to fill the sample cell, the syringe needle is inserted into the cell so that the tip is just above the bottom of the cell and the plunger is slowly lowered until the macromolecule solution appears in the overflow reservoir [22]. Then, the solution is abruptly pumped in and out of the cell to force out any trapped air bubbles from the cell. Before starting the titration, ITC needs to equilibrate. Once the signal is stable enough, the titration can begin.

For each interaction, three different background measurements should be made before the actual interaction titrations: (i) instrument blank, i.e., the titration of buffer into the buffer; (ii) heat change caused by the dilution of the macromolecule, i.e., the titration of the buffer into macromolecule; and (iii) heat change caused by the dilution of polyphenol, i.e., the titration of polyphenol into the buffer [19]. Typically, control experiments of buffer into buffer and buffer into macromolecule produce very small heat changes and only the dilution of polyphenols results in significant heat changes that need to be taken into account in the data analysis, as discussed later. In addition to control experiments, multiple replicates help to assess reproducible and precise data providing a solid basis for data processing. All interactions involve heat changes: in endothermic processes, the heat is absorbed, and in exothermic processes, the heat is released. If there is no binding heat detected, it is possible that there is no binding or interaction. Most probably, in this case, the heat change in the binding is just too low, i.e., the binding enthalpy is lower than expected, and/or the binding affinity is weaker than expected. ITC is less effective for studying interactions with very low binding affinities and small heat changes. To increase the heat change per injection, the concentrations of the macromolecule and/or polyphenol need to be increased. Conversely, the interaction can also be too strong so that all binding sites are immediately saturated within the first injection and no thermodynamic data are obtained. Also in this case, the concentrations and conditions need to be adjusted. Possible changes include decreasing or increasing the injection volume or altering experimental conditions, such as temperature, buffer composition, or pH of the buffer used.

The purity of the polyphenol samples is crucial for accurate ITC measurements. Impurities, inconsistencies in the sample preparation, or incorrect determination of molecular weight can lead to misleading results. Some polyphenols, such as flavonoids and HTs, can be easily isolated from the plant materials as individual pure compounds, in which case their molecular weight is well-known, and molar concentrations can be used. However, for oligo- and polymeric PAs, the isolation and purification process is not that straightforward, and at best, PAs can be purified as well-defined fractions [36] with their molecular weight estimated based on their mean degree of polymerization [27,37–39]. The concentrations used should be determined as accurately as possible, especially for polyphenols, as errors in these values affect the determination of the thermodynamic parameters *Ka* and ΔH [19].

Cleaning of the sample syringe and cell is crucial for successful titrations. Before each analysis, it should be verified that the instrument is clean and ready for use. This can be done by performing a water-into-water titration and/or by using commercially available test kits, such as the Ca^{2+}/EDTA test [15,40]. Results should always be within specifications; if not, the instrument is not clean. A carefully tested and optimized cleaning protocol helps to reduce run-to-run contamination. Insufficient cleaning can lead to difficulties in filling the sample cell without air bubbles, increased baseline noise, large baseline shifts, large background heat, inaccurate results, or impossible data fitting. These problems are typically well troubleshooted in the instrument manuals. However, special attention needs to be paid to cleaning the sample cell, whose cleanliness cannot be visually checked, especially in the case of "sticky" tannins. These cleaning conditions or procedures are not typically included in publications, but I strongly recommend careful routine cleaning after each analysis and more vigorous cleaning periodically or when the polyphenol or macromolecule studied is changed. This may involve using strong detergents, such as 20% Contrad 70, combined

with heating up to 50–70 °C and soaking for half an hour or even overnight if needed. After thorough cleaning, extra care should be paid at the rinsing of the sample cell in order to remove any detergent residues. Whenever the data does not match expectations, the cleanliness of the sample cell should be rechecked.

In general, ITC is considered a fast technique, especially with fully automated systems [20,21]. However, in practice, it can be rather slow due to the long equilibration time before the titrations, the high number of injections, and the delay between the injections, making the analysis time for one interaction rather long. For example, the measurement of the interaction between one specific HT and one specific protein, taking into account all equilibration times, cleaning, water-into-water titrations, control measurements, and actual interaction titrations with at least three replicates [29], took two full working days.

2.2. Data Analysis

ITC data analyses are typically performed using software or built-in programs provided by the instrument manufacturer. However, in theory, the data could be processed with any scientific data analysis software available for graphing [12,16]. Origin software (at least versions 2.9, 4.1, 5.0, 6.0 and 7.0), for instance, fits the data collected by nonlinear least-squares methods [41–43]. The Levenberg–Marquardt algorithm can be employed to determine the best-fit parameters [44,45]. An important value in this fitting process is the Chi squared (Chi^2 or χ^2) value, which the equation is trying to minimize. The χ^2 needs to be smaller than the critical values for the appropriate degrees of freedom; the smaller the χ^2 value, the better the fit. TA Instruments offers NanoAnalyze software, whose use in data fitting has been presented in detail by Srivastava and Yadav [12], and whose versions, such as 2.4.1. [28,29] and 3.12.0 [7], have been used for the data analysis of polyphenol interactions. When using this software, it is also important to check the reliability and statistics of the modeled data, maintaining a standard deviation of 0.1 and confidence level of 99% with 1000 trials [12]. However, as Freire et al. [46] have noted "statistical fitting of the data to a model does not validate the appropriateness of the model". Therefore, extra thermodynamic information is often required for a more comprehensive understanding of complex binding systems and precise binding mechanism.

In the actual data analysis, the raw data are first processed in order to correct the baseline, integrate the areas of the heat pulses, and normalize for concentration to produce a binding isotherm of a ΔH vs. molar ratio. In addition, the heat produced from necessary control measurements needs to be subtracted, such as the heat from dilution. Finally, the processed data are fitted using an appropriate binding model. The process of data fitting consists of several steps: (i) testing and selection of the model to be used; (ii) initial guesses of proper parameters to start the fitting; typically, the default variable minimum and maximum are useful, but it is important to ensure that there is a sufficiently high maximum value for stoichiometry, especially in tannin-protein interactions; (iii) the actual fitting and improvement of the initial values; and (iv) iteration of all steps until there is no further improvement of the values. If the data fitting is not successful, other possible models should be tested. If the interaction is weak, it may not be possible to fit that data reliably.

Mathematical models and equations have been devised throughout the decades, and there are many possible models to fit the data. The most widely used is the multiple sets of independent binding sites model [22,47]. The simplest model possible is the 1:1 interaction model, where one ligand molecule binds to one macromolecule. Under ideal conditions, where the titrand concentration and binding affinity are high enough, the simple 1:1 interaction will show an inflection point in the binding isotherm, and the curve will be symmetric around that inflection point [15,22]. Any asymmetry detected indicates more complex interactions, which is characteristic of polyphenol–macromolecule associations.

The most commonly used models in polyphenol–macromolecule interactions are the models for one independent set of binding sites (one-site model, also known as single-site model) and two independent sets of binding sites (two-site model). The one-site model assumes that all binding sites in the molecules are identical and independent. The two-site model presupposes that there are two distinct types of binding sites. For a complete explanation of these models, see [47].

In addition, there can be cases where more than two sets of binding sites or cooperative interactions are present [31,47,48]. Cooperative interactions, where binding occurs via sequential filling of binding sites, i.e., the binding of one ligand to a macromolecule affects the binding affinity of additional ligands, can be studied using the sequential binding model. This model determines the stepwise binding constants and enthalpy changes for each binding event [46,49]. The competitive binding model is used when two ligands with different affinities compete for the same binding site on a macromolecule [41,50]. It helps in understanding the competitive interactions and determining the binding affinities of each ligand. Other common models used for data fitting are dissociation and enzyme kinetics models. The dissociation model is used to study the dissociation of complexes, providing insights into the stability of the complex and the thermodynamic parameters associated with the dissociation process [51]. The enzyme kinetics model is used to study the interactions between enzymes and their substrates or inhibitors, determining kinetic parameters using either the Michaelis–Menten or Lineweaver–Burk methods [50].

Traditional models often include specific assumptions about binding, such as the number of binding sites and their interactions. For more complex binding scenarios, standard models are not sufficient; instead, specific models tailored to the complex interactions in the experiments may be needed. For an example, an algorithm for nonlinear regression analysis of a multiple binding site model can model up to four overlapping binding processes [45]. Another example is the differential binding model introduced by Herrera and Winnik [52]. This model uses a general set of model-independent differential equations to fit ITC data. It starts with a general assumption based on the binding polynomial of a homotropic binding system, describing the distribution of receptor-containing binding species in solution. By implicitly differentiating a mass-balance equation expressed in terms of the binding polynomial, a general set of differential equations is derived, allowing for unconstrained interactions among the binding sites [52].

In some cases, various binding models yield nearly identical fits to experimental data, making it challenging to determine which model is correct [53]. Also, the possible statistical errors in ITC data analysis and their effects on the determination of thermodynamic parameters must be taken into account, as previously discussed [54,55]. Sometimes, the measured data cannot be reliably fitted, in which case it may be justified to draw conclusions qualitatively to avoid overinterpretation of the data. For example, no clear estimates were obtained for K and n for the binding between sunflower proteins and polar phenolic acid, i.e., chlorogenic acid [56].

However, the goal is that ITC data fits provide K, n and ΔH, allowing the determination of ΔG from the binding constant:

$$\Delta G = -RTlnK, \tag{2}$$

where R is the universal gas constant and T is the absolute temperature in Kelvin. Entropy ΔS can be determined based on the second law of thermodynamics at constant temperature and pressure:

$$\Delta G = \Delta H - T\Delta S, \tag{3}$$

In general, Δ*H* values obtained are more reliable than *K* and Δ*S* values, which depend on the mathematical fitting model and experimental conditions used [57]. The Δ*H* value can also be visually checked by comparing the value given by the model to the actual isotherm. In order to use Equation (3), it is essential that the binding is reversible and that the equilibrium is reached, meaning that the peak returns to the baseline between the injections [55,58].

3. Polyphenols and Proteins

The application of ITC in studies on polyphenol–macromolecule interactions has been most popular in protein interactions and particularly in tannin–protein interactions. These interactions typically produce strong signals and distinctive titration curves [30]. The negative side is that the interpretation of the data can be challenging if tannins cannot be purified as single compounds, and, therefore, ITC is performed with plant-based tannin fractions. Model proteins in these studies have included globular proteins, such as bovine serum albumin (BSA), which is the most intensively studied model protein [18,26,28–30,59,60], and ribulose-1,5-biphosphate carboxylase oxygenase (rubisco), which is the major protein in green plants [59]. Other model proteins include proline-rich gelatin, which has an open random coil conformation [18,26,29,60], and poly(L-proline) [31]. Examples of the interactions of gemin A and geraniin with gelatin are presented in Figure 3.

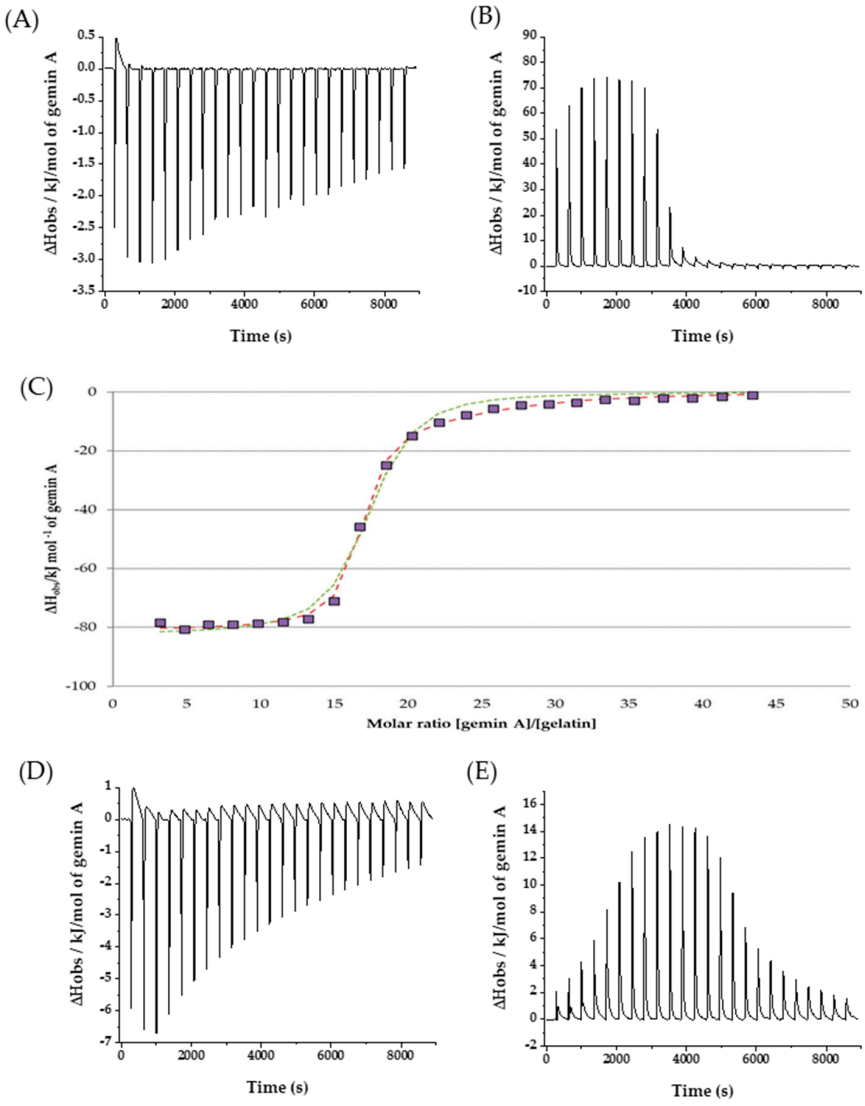

Figure 3. *Cont.*

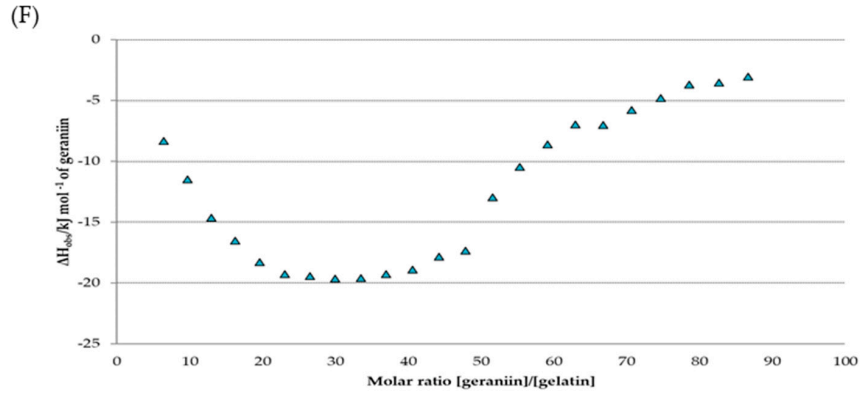

Figure 3. Examples of strong interaction showing raw data of (**A**) gemin A into buffer control titration, (**B**) gemin A into 20 μM gelatin titration, and (**C**) one-site (green dashed line) and two-site (red dashed line) binding models fitted to experimental data of this interaction; and of weaker interaction showing raw data of (**D**) geraniin into buffer control titration, (**E**) geraniin into 10 μM gelatin titration, and (**F**) binding isotherm for this interaction [29]. Exothermic reactions are shown up. Figure 3C,F are reprinted with permission from Ref. [29], *Ellagitannins with glucopyranose cores have higher affinities to proteins than acyclic ellagitannins by isothermal titration calorimetry*, Maarit Karonen, Marianne Oraviita, Irene Mueller-Harvey, Juha-Pekka Salminen, and Rebecca J. Green, Journal of Agricultural and Food Chemistry 2019, 67 (46), 12730–12740, DOI: 10.1021/acs.jafc.9b04353. Copyright © 2019 American Chemical Society.

Polyphenol–protein interactions are affected by temperature, pH, solvent composition, and the concentrations of polyphenols and macromolecules. As mentioned above, blank experiments of buffer-into-buffer and buffer-into-macromolecule produce very small heat changes and, typically, only polyphenol-into-buffer titration, i.e., the dilution of polyphenols, results in significant heat changes that need to be taken into account. In the case of tannins, self-association into aggregates occurs due to their hydrophobicity in the titration syringe, and during the injections into the sample cell, an endothermic process of deaggregation of tannins happens [27,59,60]. This can be explicitly seen from the thermograms of tannin-into-buffer titration presented in Figure 3A,D for gemin A and geraniin, respectively. The extent of deaggregation is inversely dependent on the tannin concentration present in the sample cell and, therefore, the subsequent injections produce fewer heat changes [60]. In any case, the control data of tannin-into-buffer always needs to be subtracted from the tannin-into-protein data.

The interaction between polyphenols and proteins is typically exothermic (as seen in Figure 3B,E), but there are a few exceptions in the literature. For example, the association between epigallocatechingallate and soy protein isolate exhibited endothermic binding with ΔH of 206 kJ/mol [61]. The interactions are accompanied by a high number of binding sites [28,29,59], suggesting that the binding of tannins to proteins could occur via a surface adsorption mechanism. This leads to the coating of the protein surface and subsequent changes in the functional properties of proteins, such as hydration and surface properties [62]. There are two main binding models used for data fitting of polyphenol–protein interactions: the above mentioned one-site and two-site models [59]. In general, both of the models fit the thermodynamic data well, as shown in Figure 3C and, therefore, the use of the simpler one-site binding model can often be justified [28]. However, in some cases, the two-site model can provide a better fit, indicating primary strong interaction sites and secondary weak interactions sites with $K_1 > K_2$ and $n_1 < n_2$ [28,29,59]. Often, the secondary interactions are much weaker and less specific than the primary ones, as seen in Table 1, which shows the estimated thermodynamic binding parameters for the interactions between different polyphenols, mainly tannins, and different proteins. The values cannot be

directly compared due to the variations in experimental design, conditions, and concentrations of interacting species. For example, the effect of conditions can be seen by comparing the thermodynamic parameters of oenothein B–BSA and gemin A–BSA interactions fitted by the two-site model (Table 1). In the earlier study [63], dimeric ETs were titrated into the sample cell using two titration events, with the syringe being filled within the run to achieve 48 injections. Whereas in the later study [29], the concentrations of ETs and BSA were adjusted so that only one titration event was performed without any additional distractions. Despite these differences, the estimated thermodynamic binding parameters in Table 1 provide a good overview on the strength and stoichiometry of polyphenol–protein interactions. They show that interaction between tannins and rubisco or gelatin are stronger than those with BSA. For example, K_1 is 1.7×10^5 and K_2 1.1×10^4 for the association between agrimoniin and gelatin whereas they are 3.6×10^4 and 6.9×10^2, respectively, for the agrimoniin–BSA interaction obtained by the two-site binding model [29]. As an exception, epicatechin has not shown any interaction with gelatin, even though it has weak interactions with BSA [26].

Table 1. Estimated thermodynamic binding parameters (n = stoichiometry, K = equilibrium binding constant, and ΔH = enthalpy change observed) for interactions between polyphenols and proteins obtained using different binding models in data fits, for the detailed experimental conditions and concentrations see the original references. BSA = bovine serum albumin. Tara and sumac tannins are mainly gallotannins. Chesnut and myrabolan tannins are mostly ellagitannins (ETs). Green tea polyphenols consist primarily of epicatechin and epigallocatechin and their gallates. Sorghum tannins are oligomeric and polymeric procyanidins. Grape seed tannins are oligomeric and polymeric procyanidins, which can be galloylated. Mimosa tannins contain oligomeric and polymeric profisetinidins and prorobinetinidins.

Interacting Species	n_1	K_1 (M^{-1})	ΔH_1 (kJ mol^{-1})	n_2	K_2 (M^{-1})	ΔH_2 (kJ mol^{-1})	Ref.
Agrimoniin–BSA (one-site model)	17	1.7×10^4	−24				[29]
Agrimoniin–BSA (two-site model)	16	3.6×10^4	−18	46	6.9×10^2	−8	[29]
Agrimoniin–gelatin (one-site model)	20	7.4×10^4	−76				[29]
Agrimoniin–gelatin (two-site model)	18	1.7×10^5	−65	52	1.1×10^4	−10	[29]
Chestnut tannins–BSA (one-site model)	18	9.0×10^2	−40				[18]
Chestnut tannins–gelatin (two-site model)	46	1.5×10^6	−22	32	1.1×10^4	−27	[18]
Epicatechin–BSA [1] (one-site model)	4	2.9×10^2	−37				[26]
Epicatechingallate–poly(L-proline) (one-site model)	7	8.1×10^4	−33				[31]
Epigallocatechingallate–poly(L-proline) (one-site model)	9	3.7×10^4	−25				[31]
Epicatechin tetramer–poly(L-proline) (one-site model)	6	3.4×10^5	−11				[31]
Gemin A–BSA (one-site model)	14	1.1×10^4	−45				[29]
Gemin A–BSA (two-site model)	14	1.6×10^4	−37	30	7.8×10^2	−8	[29]
Gemin A–BSA (two-site model)	13	1.8×10^6	−47	25	6.3×10^4	−11	[63]

Table 1. *Cont.*

Interacting Species	n_1	K_1 (M^{-1})	ΔH_1 (kJ mol^{-1})	n_2	K_2 (M^{-1})	ΔH_2 (kJ mol^{-1})	Ref.
Gemin A–gelatin (one-site model)	16	4.2×10^5	−81				[29]
Gemin A–gelatin (two-site model)	15	1.3×10^6	−64	21	4.2×10^4	−17	[29]
Grape seed tannins–BSA (one-site model)	7	1.5×10^3	−102				[27]
Grape seed tannins–gelatin (one-site model)	35	3.3×10^5	−38				[27]
Green tea polyhenols–BSA (one-site model)	19	1.4×10^2	−154				[27]
Green tea polyphenols–gelatin (one-site model)	71	9.8×10^3	−46				[27]
Lambertianin C–BSA (one-site model)	11	1.1×10^5	−28				[29]
Lambertianin C–BSA (two-site model)	11	1.6×10^5	−25	37	3.1×10^3	−3	[29]
Lambertianin C–gelatin (one-site model)	11	1.5×10^6	−93				[29]
Lambertianin C–gelatin (two-site model)	11	1.9×10^6	−91	15	2.5×10^2	−22	[29]
Macrocyclic tetrameric ET–BSA (one-site model)	9	2.7×10^4	−69				[28]
Macrocyclic tetrameric ET–BSA (two-site model)	9	7.3×10^4	−52	90	1.8×10^2	−19	[28]
Macrocyclic pentameric ET–BSA (one-site model)	9	2.3×10^4	−80				[28]
Macrocyclic pentameric ET–BSA (two-site model)	9	7.7×10^4	−56	35	2.6×10^2	−44	[28]
Macrocyclic hexameric ET–BSA (one-site model)	10	1.7×10^4	−88				[28]
Macrocyclic hexameric ET–BSA (two-site model)	9	5.6×10^4	−63	59	1.2×10^2	−59	[28]
Macrocyclic heptameric ET–BSA (one-site model)	10	1.7×10^4	−93				[28]
Macrocyclic heptameric ET–BSA (two-site model)	9	3.5×10^4	−73	84	1.7×10^2	−27	[28]
Mimosa tannins–BSA (one-site model)	39	5.9×10^3	−10				[27]
Mimosa tannins–gelatin (one-site model)	34	8.6×10^4	−35				[27]
Myrabolan tannins–BSA	178						[60]
Myrabolan tannins–BSA (one-site model)	22	7.0×10^2	−58				[18]
Myrabolan tannins–gelatin (two-site model)	36	2.2×10^6	−28	39	8.3×10^3	−31	[18]
Oenothein B–BSA (one-site model)	12	5.7×10^3	−14				[28]
Oenothein B–BSA (two-site model)	6	9.8×10^3	−14	36	1.1×10^3	−7	[28]
Oenothein B–BSA (two-site model)	4	6.5×10^5	−21	20	3.3×10^4	−10	[63]
Oenothein A–BSA (one-site model)	11	7.6×10^3	−45				[28]
Oenothein A–BSA (two-site model)	11	1.2×10^4	−33	32	3.5×10^2	−9	[28]
Pedunculagin–BSA (two-site model)	2	4.2×10^4	−11	30	1.1×10^3	−5	[63]

Table 1. *Cont.*

Interacting Species	n_1	K_1 (M^{-1})	ΔH_1 (kJ mol^{-1})	n_2	K_2 (M^{-1})	ΔH_2 (kJ mol^{-1})	Ref.
Pentagalloylglucose–BSA (two-site model)	17	2.2×10^5	−38	67	6.0×10^2	−49	[18]
Pentagalloylglucose–BSA (two-site model)	26	1.8×10^5	−29	26	8.0×10^2	−29	[59]
Pentagalloylglucose–BSA (one-site model)	26	2.3×10^4	−40				[59]
Pentagalloylglucose–gelatin (two-site model)	31	2.8×10^5	−47	60	7.5×10^2	−44	[18]
Pentagalloylglucose–rubisco (two-site model)	204	1.2×10^6	−35	406	3.1×10^4	−20	[59]
Pentagalloylglucose–rubisco (one-site model)	466	1.3×10^4	−37				[59]
Procyanidin tetramer–BSA (one-site model)	53	6.3×10^3	−11				[30]
Procyanidin pentamer–BSA (one-site model)	34	1.0×10^4	−13				[30]
Procyanidin hexamer–BSA (one-site model)	21	1.7×10^4	−21				[30]
Procyanidin heptamer–BSA (one-site model)	18	1.1×10^4	−27				[30]
Procyanidin octamer–BSA (one-site model)	18	1.4×10^4	−24				[30]
Roburin A–BSA (two-site model)	2	2.3×10^5	−15	16	1.8×10^4	−8	[63]
Roshenin C–gelatin (one-site model)	30	1.7×10^4	−57				[29]
Roshenin C–gelatin (two-site model)	24	1.5×10^5	−30	30	4.2×10^4	−57	[29]
Sanguiin H-6–BSA (one-site model)	19	1.3×10^4	−26				[29]
Sanguiin H-6–BSA (two-site model)	17	3.5×10^4	−18	94	1.1×10^3	−6	[29]
Sanguiin H-6–gelatin (one-site model)	17	7.3×10^4	−78				[29]
Sanguiin H-6–gelatin (two-site model)	16	2.2×10^5	−63	38	4.2×10^4	−12	[29]
Sorghum tannins–BSA (one-site model)	11	3.3×10^4	−21				[27]
Sorghum tannins–gelatin (one-site model)	16	2.0×10^6	−60				[27]
Sumac tannins–BSA (two-site model)	9	1.7×10^5	−30	24	2.2×10^3	−30	[18]
Sumac tannins–gelatin (two-site model)	35	6.9×10^5	−38	21	4.2×10^2	−49	[18]
Tara tannins–BSA	48						[60]
Tara tannins–BSA (two-site model)	3	1.0×10^4	−33	15	6.8×10^2	−25	[18]
Tara tannins–gelatin (two-site model)	53	8.0×10^3	−21	58	1.5×10^2	−21	[18]
Tellimagrandin I–BSA (one-site model)	6	1.8×10^4	−24				[28]
Tellimagrandin I–BSA (two-site model)	6	2.2×10^4	−20	4	1.8×10^3	−10	[28]
Tellimagrandin I–gelatin (one-site model)	67	7.6×10^3	−39				[29]
Tellimagrandin I–gelatin (two-site model)	52	1.8×10^5	−14	120	8.9×10^4	−11	[29]

Table 1. *Cont.*

Interacting Species	n_1	K_1 (M^{-1})	ΔH_1 (kJ mol^{-1})	n_2	K_2 (M^{-1})	ΔH_2 (kJ mol^{-1})	Ref.
Tellimagrandin II–BSA (one-site model)	30	7.3×10^3	−37				[29]
Tellimagrandin II–BSA (two-site model)	29	8.3×10^3	−33	110	3.6×10^1	−28	[29]
Tellimagrandin II–gelatin (one-site model)	31	7.6×10^4	−59				[29]
Tellimagrandin II–gelatin (two-site model)	31	8.4×10^4	−56	59	7.1×10^3	−3	[29]
Vescalagin–BSA (two-site model)	3	5.2×10^4	−8	30	1.1×10^3	−7	[63]

[1] The data are shown for the lowest BSA concentration used in the study.

In general, the polyphenol–protein interactions, especially tannin-protein interactions, exhibit high binding stoichiometries (Table 1). For example, in pentagalloylglucose–BSA interactions, n_1 is 26 for the stronger and more specific binding site and n_2 is also 26 for the second weaker and less specific binding site, indicating that a total of 52 pentagalloylglucose molecules could be bound to BSA which is consistent with the surface area calculations, suggesting that BSA 40-120 pentagalloylglucose moieties could be accommodated on the BSA surface [59]. The molecular size of the polyphenol affects its association with proteins (Table 1). It can also be seen that the interaction is weak for the flavan-3-ols and increases as the PA size increases [26,30,31]. The effects of the oligomeric size on the tannin–protein interactions have been studied by using a series of purified procyanidin oligomers [30] or oligomeric ETs [28,29]. In the case of procyanidin oligomers, ΔH increased as the molecular size increased, while the number of binding sites decreased, indicating that larger procyanidins, having more proton donors, saturate a larger proportion of protein surface [30]. In the case of ETs, the exact same phenomenon was not observed: ΔH increased as the oligomer size increased, but the number of binding sites remained the same [28]. The oligomeric ETs used contained a macrocyclic part, and based on the trends observed for the ΔH and equilibrium binding constants, it was suggested that first this macrocyclic part of ET binds to the defined binding sites on the protein surface, while the so-called flexible tail of the oligomeric ET coats the rest of protein surface [28]. This in turn highlights the importance of molecular flexibility in addition to molecular size. For ETs, it has also been noted that acyclic ETs have weaker interactions with proteins than those with glucopyranose cores, while the presence of free galloyl groups makes the interactions stronger [29]. In addition, geraniin–gelatin interaction has shown an interesting biphasic shape of the isotherm, as shown in Figure 3F [29]. Typically, interactions between tannins and proteins decrease with increasing injections of tannins as the binding sites of the proteins become saturated, as seen in gemin A–gelatin interactions in Figure 3B. But in the case of geraniin and gelatin (Figure 3E), the interaction becomes stronger with increasing injections of geraniin suggesting the initial binding being cooperative, where prebound geraniin enhances the exothermicity of the interaction [29]. Biphasic binding isotherms have also been observed in situations where the ligand induces protein oligomerization [64]; so, considering the structure of gelatin, it is plausible that geraniin can modify gelatin's secondary structure and facilitate its oligomerization [29]. Cooperativity has also been reposted also for procyanidin-α-lactalbumin/lysozyme interactions [44]. Moreover, it has been proposed that cooperative binding is not always due to the changes in protein structure. Instead, a simpler explanation could be that the initial interaction is driven by a combination of exothermic hydrogen bonding and endothermic hydrophobic interactions, while later stages are primarily influenced by exothermic hydrogen bonding [30].

In addition, an important structural feature of polyphenols seems to be the presence of galloyl groups. Although interactions are weak for flavan-3-ols, their galloylation enhances their interactions with proteins [31]. Stronger interactions have also been observed for ETs with free galloyl groups [29,63]. For tannins, the structural flexibility is important, as greater conformational flexibility enhances tannin–protein binding [18,59,60]. It is possibly this flexibility that enables tannins to function more effectively as multidentate ligands and cross-linkers, as suggested for tara tannins [60].

The thermodynamics of protein associations was reviewed by Ross and Subramanian over 40 years ago [65], and this review, which has received thousands of citations, is still widely used to explain the driven forces behind protein interactions. As seen in Figure 4, if both ΔH and ΔS are negative, hydrogen bonding and van der Waals interactions are the driving forces. If ΔS is positive, hydrophobic interactions are present. Negative ΔS suggests enhanced molecular order, which could arise during aggregation, and may also indicate that hydrogen bonding plays a part in complex formation [26]. The change in ΔG is negative in spontaneous biomolecular reactions, as observed in several cases of polyphenol–protein interactions [26,27] and other biomacromolecule interactions [16,66–69]. Both polyphenols and macromolecules are diverse groups of compounds with complex structures, resulting in various interactions with different driving forces, making it challenging to interpret ITC data accurately. Dai et al. [70] has reported spontaneous enthalpy-driven interactions between PAs and pea proteins, dominated by hydrogen bonding and van der Waals interactions (ΔH, ΔS, $\Delta G < 0$). Similar interactions have been reported in the associations between rice proteins and epigallocatechingallate [71], and gallic acid, a simple phenolic compound [72]. Previous work by Frazier et al. [27] has shown that interactions between sorghum or mimosa tannins and BSA are entropically driven ($\Delta S > 0$), suggesting the hydrophobic interactions are dominant in the complex formation, whereas the interaction with gelatin is enthalpically driven. Spontaneous entropy-driven hydrophobic interactions have also been reported for catechin and soy protein isolates (ΔH, $\Delta S > 0$, $\Delta G < 0$) [73]. Additionally, McRae et al. [74] and Kilmister et al. [30] have shown for the interactions between cocoa procyanidins and BSA and grapeseed procyanidins and polyproline, respectively, that simultaneous hydrogen bonding and hydrophobic interactions can be present. This is true not only for tannin mixtures, but also for purified tannins. They emphasized that if competing endothermic and exothermic components are present, the calculated ΔH is a sum of two opposite value and, therefore, the calculated ΔS should be treated with caution [30]. Since ΔH of binding is temperature-dependent for hydrophobic interaction-driven binding, the hydrophobic interaction can be differentiated from hydrogen bonding driven interaction by using a range of temperatures in ITC titrations [74]. When discussing polyphenol interactions, π-π stacking must be mentioned even though it has not been covered in the context of the ITC studies. This attractive and direct noncovalent interaction between aromatic moieties plays a role in polyphenol interactions: π-π stacking can occur intramolecularly or intermolecularly between polyphenols or between polyphenols and proteins [75–79]. For instance, molecular mechanics and NMR spectroscopic studies on flavan-3-ols and procyanidin dimers have shown that these polyphenols can adopt conformations that favor π-π stacking, such as the arrangement between the aromatic gallate and catechol rings of dimeric procyanidin gallates [76]. On the other hand, stacking can occur between planar phenolic rings and proline rings [77,80,81].

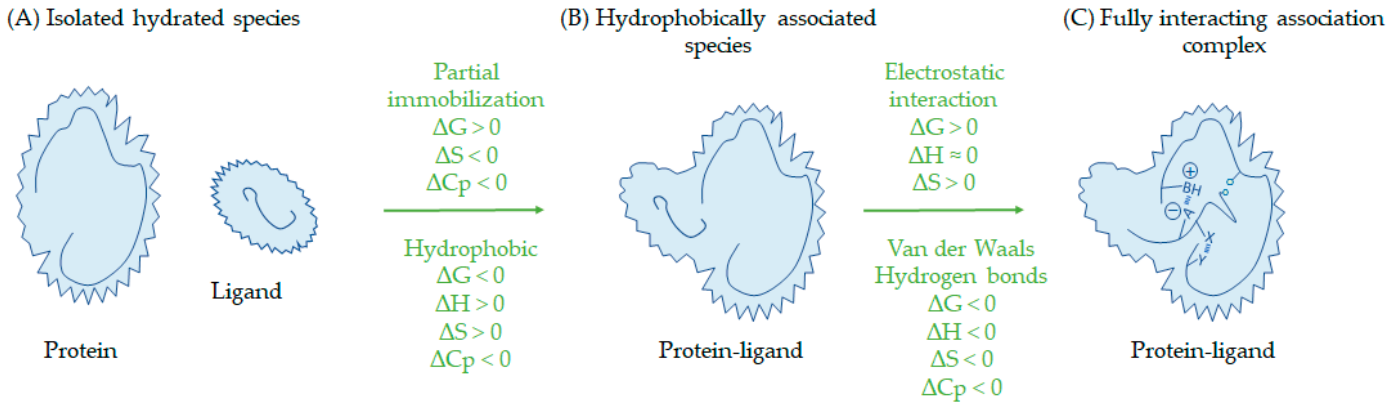

Figure 4. Adaptation of the hypothetical thermodynamic model of the protein reacting with ligand [65]: (**A**) isolated hydrated species, (**B**) partial interact with mutual penetration of their hydration layers, and (**C**) fully interacting association complex. The first step includes partial immobilization and hydrophobic association and the second step all other intermolecular interactions (ionic interactions, hydrogen bonds, and van der Waals interactions). As in the initial scheme, the irregular surrounding outlines of protein and ligand expresses ordered domain of water in comparison to other solvents. Adapted with permission from Ref. [65], *Thermodynamics of protein association reactions: forces contributing to stability*, Philip D. Ross and S. Subramanian, Biochemistry, 1981, 20 (11), 3096–3102, DOI: 10.1021/bi00514a017. Copyright © 1981 American Chemical Society.

4. Polyphenols and Polysaccharides

In comparison to polyphenol–protein interactions, ITC has been used much less in studies on polyphenol–polysaccharide interactions. However, there is an increasing number of studies in the literature where quantitative thermodynamic information has been obtained by using ITC, for example, for interactions between polyphenols and cyclodextrin [82,83], pectins [33,68,69,84,85], and cellulose [86] (example structures of which are presented in Figure 5), and wheat starch [87]. In some of the studies discussed below, tannic acid has been used as a model for polyphenols, presuming its molecular weight to be 1701 Da and its structure to have an average of 10 esterified galloyl groups, i.e., decagalloylglucose. Nevertheless, tannic acid is a mixture of many polyphenols, and its composition varies according to manufacturer and batch or manufacturing lot [88]. Therefore, the composition of the tannic acid used and the impurities present should be checked by LC-DAD or LC-MS for each batch prior to its use in ITC titrations. In discussions and conclusions, it should be pointed out that the results are not due to the interaction of a single compound, but of the different compounds in the tannic acid mixtures.

Pectins have the ability to associate with polyphenols in solutions, and these pectin-polyphenol interactions are interesting, as they affect the sensation of astringency of fruit juices and wines [3]. Watrelot et al. [33,84] have studied the interactions between pectic compounds and procyanidins by ITC using commercial apple and citrus pectins, hairy regions of pectins, rhamnogalacturonans II, arabinogalactan-proteins, and two polymeric procyanidin fractions with mean degrees of polymerization of 9 (DP9) and 30 (DP30) and the proportions of epicatechin as monomeric units 88% and 95%, respectively. The interactions observed are exothermic in nature with binding constants varying from a low association constant of 62 up to 2.6×10^3 M^{-1} and reaction enthalpies from -3 to -67 kJ/mol [33]. In general, the strength of the interactions depends on the structural and conformational factors of both the tannins and pectins [33,84]. The associations are thought to be driven by either enthalpy, as in the case of the interaction between hairy regions and shorted procyanidin oligomers DP9, or entropy, as in case the of the interaction between rhamnogalacturonan oligomers and higher procyanidin oligomers DP30, or both. This

indicates that pectic compounds and procyanidins can interact by different mechanisms, depending on the neutral sugar composition and the structure of pectins [33]. In general, the associations are slightly stronger for higher procyanidins in DP30 than for smaller ones in DP9 for commercial apple and citrus pectins [84], but the same was not observed for modified hairy regions [33]. A higher degree of polymerization has also been found to enhance the interactions between persimmon PAs and highly methylated pectins [86]. In addition, this interaction was enhanced by the presence of gallate moieties and A-type linkage in PA structures, but it also depended on the structural and conformational properties of pectins [85]. The role of arabinan side chains in pectic polysaccharides has been studied by Fernandes et al. [69], who discovered that linear arabinans have higher associations with chlorogenic acid, phloridzin, and procyanidins than the branched arabinans, but concluded that the structure of the whole polysaccharide is more important than a single part. In general, ITC studies on polyphenol–pectin interactions produce very classical binding isotherms, where a continuous decrease in the heat released is observed until the binding sites are fully saturated producing data that can be fitted with classical fitting models [33,84].

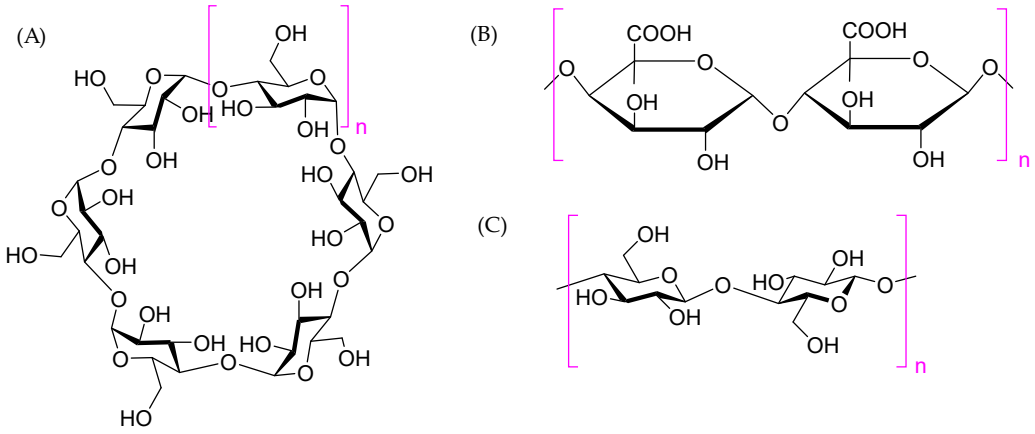

Figure 5. Model polysaccharides exhibiting associations with polyphenols: (**A**) cyclodextrins consisting of α-(1→4)-linked cyclic oligosaccharides of which as examples α-cyclodextrin (*n* = 1) and β-cyclodextrin (*n* = 2), (**B**) pectins, rich in galacturonic acid, of which as an example homogalacturonans having the linear chains of α-(1→4)-linked D-galacturonic acid units, and (**C**) cellulose consisting of the linear chains of β-(1→4)-linked D-glucose units, *n* can vary from a few hundreds to many thousands.

Fernandes et al. [68] has studied the interactions between anthocyanins and four different citrus pectic fractions by using cyanidin-3-*O*-glucoside as a model. The binding was the strongest between cyanidin-3-*O*-glucoside and low methyl esterified fractions (30% homogalacturonans, $Ka = 2.5 \times 10^4$ M^{-1}) and decreased in the following order: amidated homogalacturonans ($Ka = 4.2 \times 10^3$ M^{-1}) > high methyl esterified fractions (70% random homogalacturonans, $Ka = 1.3 \times 10^3$ M^{-1}) > high methylated esterified pectic fractions with 70% blockwise homogalacturonans ($Ka = 6.2 \times 10^2$ M^{-1}) obtained at pH 3.4 by the one-site binding model [68]. The interaction between anthocyanins and pectic polysaccharides is even more complex than with other polyphenols, as the exact structure of anthocyanin is pH-dependent: the flavylium cation is the predominant species at very acidic pH and at increasing pH, other species, such as quinoidal base and chalcone are formed [89]. For anthocyanin–pectin interactions determined at pH 3.4, electrostatic interactions might be an important mechanism, as positively charged flavylium cations and negatively charged pectic polysaccharides are present [68]. This observation for charged anthocyanins contrasts with those obtained, for example, for persimmon PAs and pectins, where cooperative hydrogen bonding and hydrophobic interactions are present, but electrostatic interactions

play no role [85]. Koh et al. [90] has studied the binding kinetics of anthocyanins with the water- and chelator-soluble pectin fractions of blueberry using Langmuir isotherms. They observed a fourfold stronger association with the more linear and more negatively charged homogalacturonan region of chelator-soluble pectins compared to the more branched, neutral-sugar-rich water-soluble pectins. The reported interaction mechanisms included hydrogen bonding, hydrophobic interactions, electrostatic interactions, and π-π stacking, depending on the pH [57,90]. The potential for π-π stacking increases under acidic conditions as anthocyanin structure transforms from non-planar to planar [90].

The interactions between tannic acid and wheat starch have shown an interesting binding isotherm exhibiting a three-step binding process, which cannot be fitted with classical fitting models [87]. In this binding process, the heat released first corresponds to the formation of soluble complexes via the associations between the compounds in tannic acid mixture and starch molecules. In the second step, the compounds in tannic acid mixture interact both with the complexes formed in the first stage and the free starch molecules, resulting in heat from both interaction and aggregation. Finally, the compounds in tannic acid act as linkers between two or more soluble complexes, generating larger insoluble complexes and even precipitation [87]. The concentration of wheat starch and the mass ratio of tannic acid to wheat starch were found to have substantial effects on the interaction. A similar stepped binding process has been reported for glucomannons: the binding between tannic acid and konjac glucomannon occurs via two stages: first the soluble complex is formed and then the aggregation takes place [91]. In this study, the raw ITC data needed to be corrected for the heat from the dilution of both tannic acid and glucomannon, but due to the complexity of the binding isotherm, the thermodynamic parameters could not be determined with the mathematical models available. Qualitatively, the associations were found to be affected by the molecular weight of glucomannon, and the pH and temperature used [91].

Another perspective on polyphenol–polysaccharide interactions is to use cell wall materials as model substances. For example, cell walls and procyanidins have been isolated from the plant materials to study cell wall polysaccharide–procyanidin interactions [92,93]. When cell walls are used as macromolecules, their concentration can be calculated, for example, as uronic acid [92] or galacturonic acid [93] acid equivalents. In general, these polyphenol-cell wall polysaccharide interactions are exothermic and produce classical thermograms, where the heat changes decrease as the procyanidin concentration increases, leading to the saturation of all binding sites [92,93]. The procyanidin-cell wall polysaccharide associations are strong with $Ka > 10^4$ M^{-1} [93], but not as strong as those presented for procyanidin–protein interactions in Table 1. Typically, the associations between cell walls and procyanidinprocyanidins involve both hydrogen bonds and hydrophobic interactions, as shown for pear procyanidins [92]. It has also been noticed that overripening affects the interactions, causing changes either in procyanidin or cell walls compositions, as procyanidin adsorption increases with ripening, and highly polymerized procyanidin are more selectively adsorbed by cell walls [92]. In addition to the previously mentioned interactions, the associations between soluble methylcellulose and epigallocatechingallate or tannic acid mixtures have also been reported to be similarly strong, exothermic, enthalpy driven, and mediated by hydrogen bonding and hydrophobic interactions [86,94]. In general, the interactions and the driving forces described above for polyphenols and polysaccharides are similar to those described for polyphenols and proteins in Section 3, i.e., exothermic and including hydrogen bonding and hydrophobic interactions.

In relation to direct polyphenol–polysaccharide interactions, there are also ITC studies on the effects of polyphenols on the cellulases, i.e., the enzymes that can degrade cellulose in plants. da Silva et al. [95] have studied the interaction between polyphenols and β-

glucosidases using tannic acid as a model, and they found the binding to be exothermic with $\Delta H < 0$ and $\Delta S < 0$. The binding was relative strong, with binding constants in the order of 10^4 M^{-1}, including hydrogen bonding but also increased hydrophobic interactions, which might be related to the release of structured water molecules from the hydrophobic surface of tannic acid [95]. Additionally, the effect of non-ionic surfactants on the interactions between cellulases and tannic acid has been studied by measuring their mutual interactions by ITC [96].

5. Polyphenols and Lipids

In comparison to polyphenol–protein/polysaccharide interactions, ITC has so far been rarely used for the studies on polyphenol–lipid interactions. However, it has been used for various interactions of model lipids with other lipids [97], proteins [42,66,98–100], peptides [101–104], metals [105,106], or surfactants [107]. The low popularity of ITC in polyphenol–lipid studies might be explained by the use of differential scanning calorimetry (DSC) for lipid membranes [108–115]. DSC measures the heat capacity of a solution as a function of temperature and allows the determination of thermodynamic properties of thermally induced transition [116,117]. Based on their characteristics, these two techniques, ITC and DSC, could be more widely used as complementary tools to provide a more comprehensive description of the thermodynamics and structure–function relationships of polyphenol–lipid interactions [117]. The model lipids studied for their polyphenol interaction are typically phospholipid membranes that self-assemble into bilayers in aqueous environments [118]; for example, 1-palmitoyl-2-oleoylphosphatidylcholine (POPC) presented in Figure 6. There are different types of liposomes, the most common ones being unilamellar and multilamellar vesicles (Figures 6B and 6C, respectively). Unilamellar vesicles can be made from multilamellar vesicles, for example, by sonication or extrusion methods. Methods for the preparation of liposomes have been reviewed in detail elsewhere [119,120].

In the few articles currently available in the literature, polyphenol–lipid interactions have been found to be rather strong and exothermic. For example, the effects of persimmon PAs on biomembrane raft domains were studied by using synthetic rafts liposomes consisting of POPC, 1-palmitoyl-2-oleoylphosphatidylethanolamine (POPE), sphingomyelin (SPM), and cholesterol (CHOL) in a 1:1:1:2 molar ratio [9]. The results showed that interactions between persimmon PAs and liposomes were driven by both hydrogen bonding (ΔH was small, i.e., −0.85 kJ/mol, but negative) and hydrophobic interactions ($\Delta S > 0$), and the binding was strong (K was 5.78×10^5 M^{-1}) [32]. Similarly, resveratrol showed a strong association with phosphatidylcholine membranes consisting of POPC, 1-palmitoyl-2-docosahexaenoylphosphatidylcholine (PDPC), and POPC/PDPC in a 2:1 ratio (mol/mol) bilayers present as large unilamellar vesicle suspensions [121]. In general, the interactions were exothermic, and the strength of resveratrol to PDPC (1.0×10^5 M^{-1}) was an order of magnitude higher than for resveratrol-POPC association (0.1×10^5 M^{-1}). Stoichiometries increased with PDPC content and were 0.5, 1.0 and 1.3 for POPC, POPC/PDPC (2:1) and PDPC, with enthalphy changes of −6.6, −5.9 and −4.6 kJ/mol, respectively [121].

Interactions of different HTs have been studied by ITC by using biomimetic lipid vesicles made from *Escherichia coli* lipid extract [7]. In this study, quantitative data were not obtained due to the lack of sigmoidal curves, but HTs were qualitative classified as (i) monomers with weak affinity for lipids: corilagin, isostrictinin, strictinin, pedunculagin, vescalagin, geraniin, chebulagic acid, chebulinic acid, and punicalagin; (ii) monomers with high affinity for lipids: trigalloylglucose, tellimagrandin I, tetragalloylglucose, casuarictin, tellimagrandin II, and pentagalloylglucose; (iii) dimers and trimers having high affinity for lipids: oenothein B, rugosin E, agrimoniin, sanguiin H-6, gemin A, rugosin D, oenothein A,

lambertianin C, and rugosin G [7]. Based on structural evaluations, the most important factors for stronger interactions were the presence of free galloyl moieties, overall structural flexibility, hydrophobicity of HT, and molecular size. However, it was noticed that hydrophobic structure alone does not guarantee an affinity for lipids, as geraniin, chebulagic acid, and chebulinic acid, did not show any detectable interactions with the lipid vesicles [7]. The observed values for ΔH varied more widely than the observed values for persimmon tannins and resveratrol above, i.e., from −80 to 0 kJ/mol of injectant and was at the same level as those observed for polyphenol–protein interactions (Table 1). The strongest interactions with lipids were observed for rugosins D and G, which are dimeric and trimeric ETs having five and seven free galloyl groups in their structures, respectively [7].

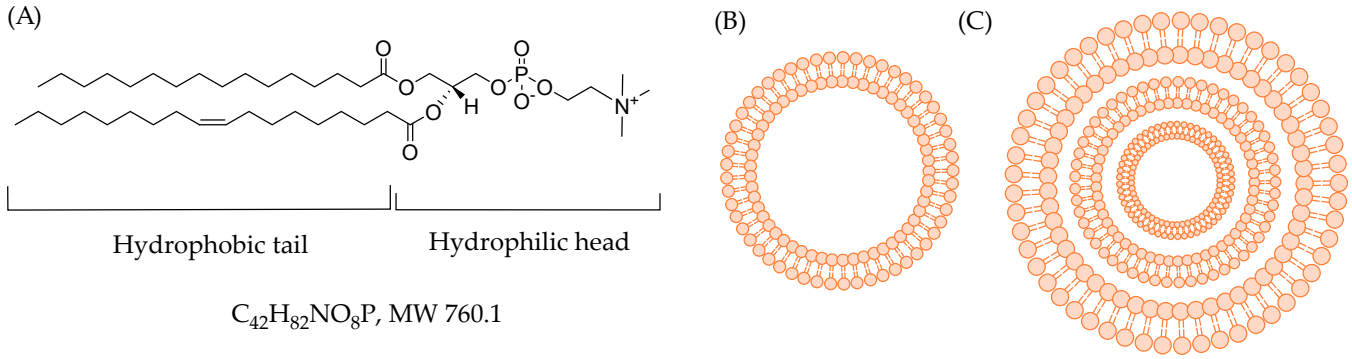

Figure 6. (**A**) 1-palmitoyl-2-oleoylphosphatidylcholine as an example of a model lipid studied for its interaction with polyphenols, (**B**) unilamellar vesicle consisting of a single phospholipid bilayer, and (**C**) multilamellar vesicle consisting of many phospholipid bilayers. The vesicles differ in scale, yet they serve as structural examples.

In addition to direct polyphenol–lipid interactions, the inhibitory effects of PAs isolated from unripe banana pulp on the cholesterol esterase, i.e., the glycoprotein belonging to the lipase/esterase family and catalyzing the conversion of ingested cholesterol esters into free cholesterol, have been studied [122]. The interaction was found to be exothermic, with a relatively strong non-covalent association with K_a of 4.44 × 10^4 M^{-1} and n of 1.12. The thermodynamic parameters ΔH, $\Delta G < 0$, and $\Delta S > 0$ indicated the binding to be spontaneous and hydrogen bonding and hydrophobic interactions the driven forces.

6. Impact on Bioavailability, Food, and Other Applications

The interactions between polyphenols and macromolecules, especially proteins and polysaccharides, impact their bioavailability, food applications, and other uses. These interactions are, therefore, of significant importance in the fields of food chemistry and processing, functional food ingredients, and human nutrition. Food processing methods, such as heat treatment and acidic conditions, affect the formation polyphenol–macromolecule complexes in plant-based food systems. Consequently, they influence the quantities of polyphenols present in the final products and their bioavailability, as reviewed elsewhere [57,123,124]. ITC could be used more extensively when the influence of both the polyphenol and macromolecule structures need to be determined in the development of functional foods or nutraceuticals so that the health benefits of polyphenols could be maximized. For example, Pripp et al. [125] has studied the interactions between phenolic compounds in olive oil and various food proteins, such as sodium caseinate (present in many fabricated foods), BSA, β-lactoglobulin, and gelatin, and their implications for bitterness perception. The phenolic compounds in olive oil had less heat impact when binding to proteins compared to tannic acid. However, the binding characteristics still allowed for an approximate prediction of how much food protein is needed to noticeably reduce

bitterness in foods containing olive oil [125]. Another example is the possibility to use plant-based polyphenol–protein complexes to form and stabilize oil-in-water emulsions [70]. Grape seed PAs and pea proteins helped stabilize oil-in-water emulsions mainly through hydrogen bonding. These complexes slightly lowered the isoelectric point, thermostability, and salt stability of the emulsion, but improved its storage stability compared to using pea proteins alone [70]. With complex sample matrices, other analytical methods are typically needed to support the ITC data. Such complementary techniques used alongside with ITC include, for example, DSC [45,56,99,119,126], dynamic light scattering techniques (DLS) [67,85,87,91,126], turbidity measurements [59,67,69,87,91,127], transmission electron microcopy (TEM) [63,85,86,91,99], X-ray photoelectron spectroscopy [87], scanning electron microscopy (SEM) [32,87,93], and rheological experiments [87,94].

Polyphenol–protein interactions have many biological effects and consequences on their activity and availability [124]. The interaction between tannins and proteins plays a role in both tanning effect and haze formations, contributing to the sensory properties, such as the bitterness and astringency experienced while enjoying beverages and food products [125]. The affinity between tannins and proteins, especially with the salivary proteins in the oral cavity, is believed to give them the astringent character recognized in tannin-rich foods, such as fruits, and beverages like apple juice, cider, beer, or wine [1,128,129]. This interaction might also be linked to the health benefits of polyphenols and their stability and absorption in the human body [123]. Polyphenol–protein interaction also impacts protein structure and quality, as well as the digestion of proteins and enzyme activity [124]. The bioactivities of polyphenol are influenced by these interactions, with both positive and negative effects reported, as reviewed elsewhere [124]. Additionally, they affect the delivery of polyphenols to the lower parts of the gastrointestinal tract; for example, thermally induced protein–epigallocatechingallate complexes have been called protective nanovehicles for epigallocatechingallate [124,130,131]. The interactions between polyphenols and polysaccharides affect the bioavailability and bioaccessibility of polyphenols [124]. This depends on how polyphenols are released from these associations. The interaction of polysaccharides with polyphenol–protein complexes also plays a role. For example, dietary carbohydrates are known to affect the interaction between procyanidin dimer B3 and trypsin by disrupting the aggregates formed [132]. Polyphenol–polysaccharide interactions can also influence the delivery of polyphenols to the lower parts of the gastrointestinal tract [124]. Microencapsulation of polyphenols into coating materials is an interesting application of this, for example, green tea catechins have been encapsulated using maltodextrin as a coating material [124,133]. The interactions between tannins and polysaccharides become significant during the food processing or chewing, or digestion as mentioned above, but also the loss of astringency in the ripening process of some fruits can be explained by polyphenol–polysaccharide interactions, as previously implied [134,135]. The affinity of polyphenols for lipid bilayers can impact their biological activity and usability. For example, the biological activities of highly polymerized and highly galloylated persimmon PAs correlated positively with their alterations on the cell membrane morphology and fluidity [65]. These results indicate that ITC could be used more to study the polyphenol–lipid interactions in health implications, such as absorption in the digestive track and interaction with cell membranes, in emulsions, and lipid-based delivery systems in food application, or in cosmetics to enhance the stability and efficacy of polyphenol-based formulations.

In order to take all interactions into account, the use of ternary ITC systems with three interacting components sounds attractive, as demonstrated in previous works by Houtman et al. [136] and Cotrina et al. [137]. However, the challenges might be that the system and experimental design can be highly sensitive to experimental conditions, the data are even more complex, the presence of multiple binding sites and potential cooperativity, and

the choice of appropriate mathematical models to fit the data. On the other hand, as the methods evolve, research possibilities will also improve. These advancements include, for example, continuous injection ITC [138,139], freely accessible ITC web calculators (e.g., [140]), and the combination of ITC with molecular modeling, molecular dynamics simulations, and machine learning methods [141–143].

7. Conclusions

ITC is an excellent tool for determining the thermodynamic parameters of polyphenol–macromolecule interactions. These interactions of polyphenols with different macromolecules, such as proteins, polysaccharide, and lipids, naturally depend on the studied polyphenol, the structure of the macromolecule and the conditions used. However, there are many similarities, such as the driving forces; often, both the hydrogen bonding and the hydrophobic interactions are present. Important structural features of polyphenols seem to be the flexibility, the number of galloyl groups and the size of the molecule or the degree of polymerization. In general, the polyphenol–macromolecule interactions are strong, which increases the reliability of data fits and the determination of the thermodynamic parameters. However, adjusting the experimental conditions and concentrations used can sometimes be challenging, and sigmoidal isotherm may not be achieved. In such cases, it might be better to interpret the results qualitatively rather than overinterpreting uncertain fitted data. In conclusion, the studies on the interactions between polyphenols and macromolecules using ITC have provided valuable insights into the thermodynamics and mechanisms of these interactions, with implications for their biochemistry, food applications, and other uses. However, challenges in understanding the exact mechanisms and addressing the effects on bioavailability and nutritional quality remain to be overcome.

Funding: This research received no external funding.

Data Availability Statement: No new data were created or analyzed in this study. Data sharing is not applicable to this article.

Acknowledgments: Rebecca J. Green is warmly thanked for introducing me to the world of ITC and for all the fruitful discussions over the years. Anne Koivuniemi and Mimosa Sillanpää are kindly thanked for their technical guides made for ITC200 and used here as notes to remember all practical tips. Mimosa Sillanpää also kindly read and commented on the first draft of manuscript.

Conflicts of Interest: The author declares no conflicts of interest.

References

1. Quideau, S.; Deffieux, D.; Douat-Casassus, C.; Pouységu, L. Plant Polyphenols: Chemical Properties, Biological Activities, and Synthesis. *Angew. Chem. Int. Ed.* **2011**, *50*, 586–621. [CrossRef] [PubMed]
2. Hagerman, A.E. Fifty Years of Polyphenol–Protein Complexes. In *Recent Advances in Polyphenol Research, Volume 3*; Cheynier, V., Sarni-Manchado, P., Quideau, S., Eds.; Wiley-Blackwell: Hoboken, NJ, USA, 2012; pp. 71–97.
3. Le Bourvellec, C.; Renard, C.M.G.C. Interactions between Polyphenols and Macromolecules: Quantification Methods and Mechanisms. *Crit. Rev. Food Sci. Nutr.* **2012**, *52*, 213–248. [CrossRef] [PubMed]
4. Le Bourvellec, C.; Renard, C.M.G.C. Non-Covalent Interaction between Procyanidins and Apple Cell Wall Material. Part II: Quantification and Impact of Cell Wall Drying. *Biochim. Biophys. Acta* **2005**, *1725*, 1–9. [CrossRef] [PubMed]
5. Padayachee, A.; Netzel, G.; Netzel, M.; Day, L.; Zabaras, D.; Mikkelsen, D.; Gidley, M.J. Binding of Polyphenols to Plant Cell Wall Analogues—Part 1: Anthocyanins. *Food Chem.* **2012**, *134*, 155–161. [CrossRef]
6. Le Bourvellec, C.; Renard, C.M.G.C. Interactions between Polyphenols and Macromolecules: Effect of Tannin Structure. *Encycl. Food Chem.* **2019**, *2*, 515–521. [CrossRef]
7. Virtanen, V.; Green, R.J.; Karonen, M. Interactions between Hydrolysable Tannins and Lipid Vesicles from *Escherichia coli* with Isothermal Titration Calorimetry. *Molecules* **2022**, *27*, 3204. [CrossRef] [PubMed]
8. Virtanen, V.; Puljula, E.; Räikkönen, S.; Karonen, M. Ellagitannin-Lipid Interaction by HR-MAS NMR. *Molecules* **2021**, *26*, 373. [CrossRef] [PubMed]

9. Scheidt, H.A.; Huster, D. The Interaction of Small Molecules with Phospholipid Membranes Studied by ^{1}H NOESY NMR under Magic-Angle Spinning. *Acta Pharmacol. Sin.* **2008**, *29*, 35–49. [CrossRef] [PubMed]
10. Scheidt, H.A.; Pampel, A.; Nissler, L.; Gebhardt, R.; Huster, D. Investigation of the Membrane Localization and Distribution of Flavonoids by High-Resolution Magic Angle Spinning NMR Spectroscopy. *Biochim. Biophys. Acta* **2004**, *1663*, 97–107. [CrossRef] [PubMed]
11. Kakiuchi, N.; Wang, X.; Hattori, M.; Okuda, T.; Namba, T. Circular Dichroism Studies on the Ellagitannins-Nucleic Acids Interaction. *Chem. Pharm. Bull.* **1987**, *35*, 2875–2879. [CrossRef]
12. Srivastava, V.K.; Yadav, R. Chapter 9—Isothermal titration calorimetry. In *Data Processing Handbook for Complex Biological Data Sources*; Misra, G., Ed.; Academic Press: Cambridge, MA, USA, 2019; pp. 125–137, ISBN 9780128165485. Available online: https://www.sciencedirect.com/science/article/pii/B9780128165485000095 (accessed on 5 September 2024). [CrossRef]
13. Wilcox, D.E. Isothermal Titration Calorimetry of Metal Ions Binding to Proteins: An Overview of Recent Studies. *Inorganica Chim. Acta* **2008**, *361*, 857–867. [CrossRef]
14. Grossoehme, N.E.; Spuches, A.M.; Wilcox, D.E. Application of Isothermal Titration Calorimetry in Bioinorganic Chemistry. *J. Biol. Inorg. Chem.* **2010**, *15*, 1183–1191. [CrossRef] [PubMed]
15. Bastos, M.; Velazquez-Campoy, A. Isothermal Titration Calorimetry (ITC): A Standard Operating Procedure (SOP). *Eur. Biophys. J.* **2021**, *50*, 363–371. [CrossRef] [PubMed]
16. Archer, W.R.; Schulz, M.D. Isothermal Titration Calorimetry: Practical Approaches and Current Applications in Soft Matter. *Soft Matter* **2020**, *16*, 8760–8774. [CrossRef] [PubMed]
17. Bastos, M.; Briggner, L.-E.; Shehatta, I.; Wadsö, I. The Binding of Alkane-α,ω-Diols to α-Cyclodextrin. A Microcalorimetric Study. *J. Chem. Thermodyn.* **1990**, *22*, 1181–1190. [CrossRef]
18. Deaville, E.R.; Green, R.J.; Mueller-Harvey, I.; Willoughby, I.; Frazier, R.A. Hydrolyzable Tannin Structures Influence Relative Globular and Random Coil Protein Binding Strengths. *J. Agric. Food Chem.* **2007**, *55*, 4554–4561. [CrossRef] [PubMed]
19. Lewis, E.A.; Murphy, K.P. Isothermal Titration Calorimetry. In *Methods in Molecular Biology: Protein-Ligand Interactions: Methods and Applications*; Humana Press: Totowa, NJ, USA, 2005; Volume 305, pp. 1–15, ISBN 9788578110796.
20. PEAQ-ITC Systems. Available online: https://www.malvernpanalytical.com/en/assets/malvern_panalytical_microcal_peaq_itc_brochure_pn12309_tcm50-23553.pdf (accessed on 21 August 2024).
21. Microcalorimetry: TA Instruments RS-DSC, DSC & ITC. Available online: https://www.tainstruments.com/pdf/brochure/TA-Instruments-RSDSC-DSC-ITC-Brochure-EN.pdf (accessed on 21 August 2024).
22. Lopez, M.M.; Makhatadze, G.I. Isothermal Titration Calorimetry. *Methods Mol. Biol.* **2004**, *173*, 121–126. [CrossRef]
23. Wiseman, T.; Williston, S.; Brandts, J.F.; Lin, L.-N. Rapid Measurement of Binding Constants and Heats of Binding Using a New Titration Calorimeter. *Anal. Biochem.* **1989**, *179*, 131–137. [CrossRef] [PubMed]
24. Biswas, T.; Tsodikov, O.V. An Easy-to-Use Tool for Planning and Modeling a Calorimetric Titration. *Anal. Biochem.* **2010**, *406*, 91–93. [CrossRef]
25. Broecker, J.; Vargas, C.; Keller, S. Revisiting the Optimal c Value for Isothermal Titration Calorimetry. *Anal. Biochem.* **2011**, *418*, 307–309. [CrossRef] [PubMed]
26. Frazier, R.A.; Papadopoulou, A.; Green, R.J. Isothermal Titration Calorimetry Study of Epicatechin Binding to Serum Albumin. *J. Pharm. Biomed. Anal.* **2006**, *41*, 1602–1605. [CrossRef] [PubMed]
27. Frazier, R.A.; Deaville, E.R.; Green, R.J.; Stringano, E.; Willoughby, I.; Plant, J.; Mueller-Harvey, I. Interactions of Tea Tannins and Condensed Tannins with Proteins. *J. Pharm. Biomed. Anal.* **2010**, *51*, 490–495. [CrossRef] [PubMed]
28. Karonen, M.; Oraviita, M.; Mueller-Harvey, I.; Salminen, J.-P.; Green, R.J. Binding of an Oligomeric Ellagitannin Series to Bovine Serum Albumin (BSA): Analysis by Isothermal Titration Calorimetry (ITC). *J. Agric. Food Chem.* **2015**, *63*, 10647–10654. [CrossRef] [PubMed]
29. Karonen, M.; Oraviita, M.; Mueller-Harvey, I.; Salminen, J.-P.; Green, R.J. Ellagitannins with Glucopyranose Cores Have Higher Affinities to Proteins than Acyclic Ellagitannins by Isothermal Titration Calorimetry. *J. Agric. Food Chem.* **2019**, *67*, 12730–12740. [CrossRef]
30. Kilmister, R.L.; Faulkner, P.; Downey, M.O.; Darby, S.J.; Falconer, R.J. The Complexity of Condensed Tannin Binding to Bovine Serum Albumin—An Isothermal Titration Calorimetry Study. *Food Chem.* **2016**, *190*, 173–178. [CrossRef]
31. Poncet-Legrand, C.; Gautier, C.; Cheynier, V.; Imberty, A. Interactions between Flavan-3-Ols and Poly(L-Proline) Studied by Isothermal Titration Calorimetry: Effect of the Tannin Structure. *J. Agric. Food Chem.* **2007**, *55*, 9235–9240. [CrossRef]
32. Zhu, W.; Wang, R.; Khalifa, I.; Li, C. Understanding toward the Biophysical Interaction of Polymeric Proanthocyanidins (Persimmon Condensed Tannins) with Biomembranes: Relevance for Biological Effects. *J. Agric. Food Chem.* **2019**, *67*, 11044–11052. [CrossRef] [PubMed]
33. Watrelot, A.A.; Le Bourvellec, C.; Imberty, A.; Renard, C.M.G.C. Neutral Sugar Side Chains of Pectins Limit Interactions with Procyanidins. *Carbohydr. Polym.* **2014**, *99*, 527–536. [CrossRef]

34. Engström, M.T.; Karonen, M.; Ahern, J.R.; Baert, N.; Payré, B.; Hoste, H.; Salminen, J.-P. Chemical Structures of Plant Hydrolyzable Tannins Reveal Their in Vitro Activity against Egg Hatching and Motility of *Haemonchus contortus* Nematodes. *J. Agric. Food Chem.* **2016**, *64*, 840–851. [CrossRef]
35. Wang, C.C.; Chen, H.F.; Wu, J.Y.; Chen, L.G. Stability of Principal Hydrolysable Tannins from Trapa Taiwanensis Hulls. *Molecules* **2019**, *24*, 365. [CrossRef]
36. Leppä, M.M.; Karonen, M.; Tähtinen, P.; Engström, M.T.; Salminen, J.-P. Isolation of Chemically Well-Defined Semipreparative Liquid Chromatography Fractions from Complex Mixtures of Proanthocyanidin Oligomers and Polymers. *J. Chromatogr. A* **2018**, *1576*, 67–79. [CrossRef] [PubMed]
37. Guyot, S.; Marnet, N.; Sanoner, P.; Drilleau, J.-F. Direct Thiolysis on Crude Apple Materials for High-Performance Liquid Chromatography Characterization and Quantification of Polyphenols in Cider Apple Tissues and Juices. *Methods Enzymol.* **2001**, *335*, 57–70. [CrossRef] [PubMed]
38. Guyot, S.; Marnet, N.; Laraba, D.; Sanoner, P.; Drilleau, J.-F. Reversed-Phase HPLC Following Thiolysis for Quantitative Estimation and Characterization of the Four Main Classes of Phenolic Compounds in Different Tissue Zones of a French Cider Apple Variety (*Malus domestica* Var. *Kermerrien*). *J. Agric. Food Chem.* **1998**, *46*, 1698–1705. [CrossRef]
39. Engström, M.T.; Pälijärvi, M.; Fryganas, C.; Grabber, J.H.; Mueller-Harvey, I.; Salminen, J.-P. Rapid Qualitative and Quantitative Analyses of Proanthocyanidin Oligomers and Polymers by UPLC-MS/MS. *J. Agric. Food Chem.* **2014**, *62*, 3390–3399. [CrossRef]
40. Ràfols, C.; Bosch, E.; Barbas, R.; Prohens, R. The Ca^{2+}-EDTA Chelation as Standard Reaction to Validate Isothermal Titration Calorimeter Measurements (ITC). *Talanta* **2016**, *154*, 354–359. [CrossRef] [PubMed]
41. Sigurskjold, B.W. Exact Analysis of Competition Ligand Binding by Displacement Isothermal Titration Calorimetry. *Anal. Biochem.* **2000**, *277*, 260–266. [CrossRef] [PubMed]
42. Swamy, M.J.; Sankhala, R.S. Probing the Thermodynamics of Protein–Lipid Interactions by Isothermal Titration Calorimetry. In *Lipid-Protein Interactions*; Kleinschmidt, J., Ed.; Methods in Molecular Biology; Humana Press: Totowa, NJ, USA, 2013; Volume 974, pp. 37–53, ISBN 9781627032759. [CrossRef]
43. Giri, P.; Pal, C. An Overview on the Thermodynamic Techniques Used in Food Chemistry. *Mod. Chem. Appl.* **2014**, *2*, 100142. [CrossRef]
44. Prigent, S.V.E.; Voragen, A.G.J.; van Koningsveld, G.A.; Baron, A.; Renard, C.M.G.C.; Gruppen, H. Interactions between Globular Proteins and Procyanidins of Different Degrees of Polymerization. *J. Dairy. Sci.* **2009**, *92*, 5843–5853. [CrossRef] [PubMed]
45. Le, V.H.; Buscaglia, R.; Chaires, J.B.; Lewis, E.A. Modeling Complex Equilibria in ITC Experiments: Thermodynamic Parameters Estimation for a Three Binding Site Model. *Anal. Biochem.* **2013**, *434*, 233–241. [CrossRef] [PubMed]
46. Freire, E.; Schön, A.; Velazquez-Campoy, A. Isothermal Titration Calorimetry: General Formalism Using Binding Polynomials. *Methods Enzymol.* **2009**, *455*, 127–155. [PubMed]
47. Freire, E.; Mayorga, O.L.; Straume, M. Isothermal Titration Calorimetry. *Anal. Chem.* **1990**, *62*, 950A–959A. [CrossRef]
48. Brautigam, C.A. Fitting Two- and Three-Site Binding Models to Isothermal Titration Calorimetric Data. *Methods* **2015**, *76*, 124–136. [CrossRef] [PubMed]
49. Menéndez, M. Isothermal Titration Calorimetry: Principles and Applications. *eLS* **2020**, *1*, 113–127. [CrossRef]
50. Freyer, M.W.; Lewis, E.A. Isothermal Titration Calorimetry: Experimental Design, Data Analysis, and Probing Macromolecule/Ligand Binding and Kinetic Interactions. *Methods Cell Biol.* **2008**, *84*, 79–113. [CrossRef]
51. Velazquez-Campoy, A.; Leavitt, S.A.; Freire, E. Characterization of Protein-Protein interactions by Isothermal Titration Calorimetry. In *Methods in Molecular Biology: 18 19 20 Protein-Protein Interactions: Methods and Protocols*; Meyerkord, C.L., Haian, F., Eds.; Springer Science+Business Media: New York, NY, USA, 2015; pp. 183–204.
52. Herrera, I.; Winnik, M.A. Differential Binding Models for Isothermal Titration Calorimetry: Moving beyond the Wiseman Isotherm. *J. Phys. Chem. B* **2013**, *117*, 8659–8672. [CrossRef]
53. Freiburger, L.A.; Auclair, K.; Mittermaier, A.K. Elucidating Protein Binding Mechanisms by Variable-*c* ITC. *ChemBioChem* **2009**, *10*, 2871–2873. [CrossRef] [PubMed]
54. Tellinghuisen, J. Statistical Error in Isothermal Titration Calorimetry. *Methods Enzymol.* **2004**, *383*, 245–281. [PubMed]
55. Pethica, B.A. Misuse of Thermodynamics in the Interpretation of Isothermal Titration Calorimetry Data for Ligand Binding to Proteins. *Anal. Biochem.* **2015**, *472*, 21–29. [CrossRef]
56. Karefyllakis, D.; Altunkaya, S.; Berton-Carabin, C.C.; van der Goot, A.J.; Nikiforidis, C.V. Physical Bonding between Sunflower Proteins and Phenols: Impact on Interfacial Properties. *Food Hydrocoll.* **2017**, *73*, 326–334. [CrossRef]
57. Liu, X.; Le Bourvellec, C.; Renard, C.M.G.C. Interactions between Cell Wall Polysaccharides and Polyphenols: Effect of Molecular Internal Structure. *Compr. Rev. Food Sci. Food Saf.* **2020**, *19*, 3574–3617. [CrossRef]
58. Falconer, R.J. Applications of Isothermal Titration Calorimetry—The Research and Technical Developments from 2011 to 2015. *J. Mol. Recognit.* **2016**, *29*, 504–515. [CrossRef]
59. Dobreva, M.A.; Frazier, R.A.; Mueller-Harvey, I.; Clifton, L.A.; Gea, A.; Green, R.J. Binding of Pentagalloyl Glucose to Two Globular Proteins Occurs via Multiple Surface Sites. *Biomacromolecules* **2011**, *12*, 710–715. [CrossRef] [PubMed]

60. Frazier, R.A.; Papadopoulou, A.; Mueller-Harvey, I.; Kissoon, D.; Green, R.J. Probing Protein-Tannin Interactions by Isothermal Titration Microcalorimetry. *J. Agric. Food Chem.* **2003**, *51*, 5189–5195. [CrossRef]
61. You, Y.; Yang, L.; Chen, H.; Xiong, L.; Yang, F. Effects of (-)-Epigallocatechin-3-Gallate on the Functional and Structural Properties of Soybean Protein Isolate. *J. Agric. Food Chem.* **2021**, *69*, 2306–2315. [CrossRef] [PubMed]
62. Spencer, C.M.; Cai, Y.; Martin, R.; Gaffney, S.H.; Goulding, P.N.; Magnolato, D.; Lilley, T.H.; Haslam, E. Polyphenol Complexation-Some Thoughts and Observations. *Phytochemistry* **1988**, *27*, 2397–2409. [CrossRef]
63. Dobreva, M.A.; Green, R.J.; Mueller-Harvey, I.; Salminen, J.-P.; Howlin, B.J.; Frazier, R.A. Size and Molecular Flexibility Affect the Binding of Ellagitannins to Bovine Serum Albumin. *J. Agric. Food Chem.* **2014**, *62*, 9186–9194. [CrossRef] [PubMed]
64. Thao, S.; Escalante-Semerena, J.C. Biochemical and Thermodynamic Analyses of *Salmonella enterica* Pat, a Multidomain, Multimeric N-Lysine Acetyltransferase Involved in Carbon and Energy Metabolism. *mBio* **2011**, *2*, 1–8. [CrossRef] [PubMed]
65. Ross, P.D.; Subramanian, S. Thermodynamics of Protein Association Reactions: Forces Contributing to Stability. *Biochemistry* **1981**, *20*, 3096–3102. [CrossRef] [PubMed]
66. Swamy, M.J.; Sankhala, R.S.; Singh, B.P. Thermodynamic Analysis of Protein-Lipid Interactions by Isothermal Titration Calorimetry. In *Lipid-Protein Interactions: Methods and Protocols, Methods in Molecular Biology*; Kleinschmidt, J.H., Ed.; Springer Science+Business Media: New York, NY, USA, 2019; Volume 2003, pp. 71–89, ISBN 9781493990658.
67. Gabriel, G.J.; Pool, J.G.; Som, A.; Dabkowski, J.M.; Coughlin, E.B.; Muthukumar, M.; Tew, G.N. Interactions between Antimicrobial Polynorbornenes and Phospholipid Vesicles Monitored by Light Scattering and Microcalorimetry. *Langmuir* **2008**, *24*, 12489–12495. [CrossRef] [PubMed]
68. Fernandes, A.; Oliveira, J.; Fonseca, F.; Ferreira-da-Silva, F.; Mateus, N.; Vincken, J.P.; de Freitas, V. Molecular Binding between Anthocyanins and Pectic Polysaccharides—Unveiling the Role of Pectic Polysaccharides Structure. *Food Hydrocoll.* **2020**, *102*, 105625. [CrossRef]
69. Fernandes, P.A.R.; Le Bourvellec, C.; Renard, C.M.G.C.; Wessel, D.F.; Cardoso, S.M.; Coimbra, M.A. Interactions of Arabinan-Rich Pectic Polysaccharides with Polyphenols. *Carbohydr. Polym.* **2020**, *230*, 115644. [CrossRef] [PubMed]
70. Dai, T.; Li, T.; Li, R.; Zhou, H.; Liu, C.; Chen, J.; McClements, D.J. Utilization of Plant-Based Protein-Polyphenol Complexes to Form and Stabilize Emulsions: Pea Proteins and Grape Seed Proanthocyanidins. *Food Chem.* **2020**, *329*, 127219. [CrossRef] [PubMed]
71. Xu, Y.; Dai, T.; Li, T.; Huang, K.; Li, Y.; Liu, C.; Chen, J. Investigation on the Binding Interaction between Rice Glutelin and Epigallocatechin-3-Gallate Using Spectroscopic and Molecular Docking Simulation. *Spectrochim. Acta A Mol. Biomol. Spectrosc.* **2019**, *217*, 215–222. [CrossRef] [PubMed]
72. Dai, T.; Yan, X.; Li, Q.; Li, T.; Liu, C.; McClements, D.J.; Chen, J. Characterization of Binding Interaction between Rice Glutelin and Gallic Acid: Multi-Spectroscopic Analyses and Computational Docking Simulation. *Food Res. Int.* **2017**, *102*, 274–281. [CrossRef] [PubMed]
73. Dai, S.; Lian, Z.; Qi, W.; Chen, Y.; Tong, X.; Tian, T.; Lyu, B.; Wang, M.; Wang, H.; Jiang, L. Non-Covalent Interaction of Soy Protein Isolate and Catechin: Mechanism and Effects on Protein Conformation. *Food Chem.* **2022**, *384*, 132507. [CrossRef]
74. McRae, J.M.; Falconer, R.J.; Kennedy, J.A. Thermodynamics of Grape and Wine Tannin Interaction with Polyproline: Implications for Red Wine Astringency. *J. Agric. Food Chem.* **2010**, *58*, 12510–12518. [CrossRef] [PubMed]
75. de Freitas, V.A.P.; Glories, Y.; Bourgeois, G.; Vitry, C. Characterisation of Oligomeric and Polymeric Procyanidins from Grape Seeds by Liquid Secondary Ion Mass Spectrometry. *Phytochemistry* **1998**, *49*, 1435–1441. [CrossRef]
76. de Freitas, V.; Mateus, N. Structural Features of Procyanidin Interactions with Salivary Proteins. *J. Agric. Food Chem.* **2001**, *49*, 940–945. [CrossRef]
77. Cala, O.; Pinaud, N.; Simon, C.; Fouquet, E.; Laguerre, M.; Dufourc, E.J.; Pianet, I. NMR and Molecular Modeling of Wine Tannins Binding to Saliva Proteins: Revisiting Astringency from Molecular and Colloidal Prospects. *FASEB J.* **2010**, *24*, 4281–4290. [CrossRef]
78. Tarascou, I.; Barathieu, K.; Simon, C.; Ducasse, M.A.; André, Y.; Fouquet, E.; Dufourc, E.J.; De Freitas, V.; Laguerre, M.; Pianet, I. A 3D Structural and Conformational Study of Procyanidin Dimers in Water and Hydro-Alcoholic Media as Viewed by NMR and Molecular Modeling. *Magn. Reson. Chem.* **2006**, *44*, 868–880. [CrossRef] [PubMed]
79. Hagerman, A.E.; Rice, M.E.; Ritchard, N.T. Mechanisms of Protein Precipitation for Two Tannins, Pentagalloyl Glucose and Epicatechin$_{16}$ (4-8) Catechin (Procyanidin). *J. Agric. Food Chem.* **1998**, *46*, 2590–2595. [CrossRef]
80. Murray, N.; Williamson, M.; Lilley, T.; Haslam, E. Study of the Interaction between Salivary Proline-Rich Proteins and a Polyphenol by ^{1}H-NMR Spectroscopy. *Eur. J. Biochem.* **1994**, *219*, 923–935. [CrossRef]
81. Luck, G.; Liao, H.; Murray, N.J.; Grimmer, H.R.; Warminski, E.E.; Williamson, M.P.; Lilley, T.H.; Haslam, E. Polyphenols, Astringency and Proline-Rich Proteins. *Phytochemistry* **1994**, *37*, 357–371. [CrossRef]
82. Gaffney, S.H.; Martin, R.; Lilley, T.H.; Haslam, E.; Magnolato, D. The Association of Polyphenols with Caffeine and α- and β-Cyclodextrin in Aqueous Media. *J. Chem. Soc. Chem. Commun.* **1986**, 107–109. [CrossRef]

83. Kríž, Z.; Koča, J.; Imberty, A.; Charlot, A.; Auzély-Velty, R. Investigation of the Complexation of (+)-Catechin by β-Cyclodextrin by a Combination of NMR, Microcalorimetry and Molecular Modeling Techniques. *Org. Biomol. Chem.* **2003**, *1*, 2590–2595. [CrossRef] [PubMed]
84. Watrelot, A.A.; Le Bourvellec, C.; Imberty, A.; Renard, C.M.G.C. Interactions between Pectic Compounds and Procyanidins Are Influenced by Methylation Degree and Chain Length. *Biomacromolecules* **2013**, *14*, 709–718. [CrossRef]
85. Mamet, T.; Ge, Z.-Z.; Zhang, Y.; Li, C.-M. Interactions between Highly Galloylated Persimmon Tannins and Pectins. *Int. J. Biol. Macromol.* **2018**, *106*, 410–417. [CrossRef] [PubMed]
86. Patel, A.R.; Seijen-ten-Hoorn, J.; Velikov, K.P. Colloidal Complexes from Associated Water Soluble Cellulose Derivative (Methylcellulose) and Green Tea Polyphenol (Epigallocatechin Gallate). *J. Colloid. Interface Sci.* **2011**, *364*, 317–323. [CrossRef] [PubMed]
87. Wei, X.; Li, J.; Li, B. Multiple Steps and Critical Behaviors of the Binding of Tannic Acid to Wheat Starch: Effect of the Concentration of Wheat Starch and the Mass Ratio of Tannic Acid to Wheat Starch. *Food Hydrocoll.* **2019**, *94*, 174–182. [CrossRef]
88. Salminen, J.-P.; Karonen, M. Chemical Ecology of Tannins and Other Phenolics: We Need a Change in Approach. *Funct. Ecol.* **2011**, *25*, 325–338. [CrossRef]
89. Pina, F.; Oliveira, J.; De Freitas, V. Anthocyanins and Derivatives Are More than Flavylium Cations. *Tetrahedron* **2015**, *71*, 3107–3114. [CrossRef]
90. Koh, J.; Xu, Z.; Wicker, L. Binding Kinetics of Blueberry Pectin-Anthocyanins and Stabilization by Non-Covalent Interactions. *Food Hydrocoll.* **2020**, *99*, 105354. [CrossRef]
91. He, Y.; Wang, S.; Li, J.; Liang, H.; Wei, X.; Peng, D.; Jiang, Z.; Li, B. Interaction between Konjac Glucomannan and Tannic Acid: Effect of Molecular Weight, PH and Temperature. *Food Hydrocoll.* **2019**, *94*, 451–458. [CrossRef]
92. Brahem, M.; Renard, C.M.G.C.; Bureau, S.; Watrelot, A.A.; Le Bourvellec, C. Pear Ripeness and Tissue Type Impact Procyanidin-Cell Wall Interactions. *Food Chem.* **2019**, *275*, 754–762. [CrossRef] [PubMed]
93. Le Bourvellec, C.; Watrelot, A.A.; Ginies, C.; Imberty, A.; Renard, C.M.G.C. Impact of Processing on the Noncovalent Interactions between Procyanidin and Apple Cell Wall. *J. Agric. Food Chem.* **2012**, *60*, 9484–9494. [CrossRef]
94. Patel, A.R.; Seijen Ten-Hoorn, J.; Hazekamp, J.; Blijdenstein, T.B.J.; Velikov, K.P. Colloidal Complexation of a Macromolecule with a Small Molecular Weight Natural Polyphenol: Implications in Modulating Polymer Functionalities. *Soft Matter* **2013**, *9*, 1428–1436. [CrossRef]
95. Da Silva, V.M.; Sato, J.A.P.; Araujo, J.N.; Squina, F.M.; Muniz, J.R.C.; Riske, K.A.; Garcia, W. Systematic Studies of the Interactions between a Model Polyphenol Compound and Microbial β-Glucosidases. *PLoS ONE* **2017**, *12*, e0181629. [CrossRef]
96. Olsen, S.N.; Bohlin, C.; Murphy, L.; Borch, K.; McFarland, K.C.; Sweeny, M.D.; Westh, P. Effects of Non-Ionic Surfactants on the Interactions between Cellulases and Tannic Acid: A Model System for Cellulase-Poly-Phenol Interactions. *Enzyme Microb. Technol.* **2011**, *49*, 353–359. [CrossRef] [PubMed]
97. Liu, D.Z.; Chen, W.Y.; Tasi, L.M.; Yang, S.P. Microcalorimetric and Shear Studies on the Effects of Cholesterol on the Physical Stability of Lipid Vesicles. *Colloids Surf. A Physicochem. Eng. Asp.* **2000**, *172*, 57–67. [CrossRef]
98. Carneiro, F.A.; Bianconi, M.L.; Weissmüller, G.; Stauffer, F.; Da Poian, A.T. Membrane Recognition by Vesicular Stomatitis Virus Involves Enthalpy-Driven Protein-Lipid Interactions. *J. Virol.* **2002**, *76*, 3756–3764. [CrossRef] [PubMed]
99. Rovere, M.; Sanderson, J.B.; Fonseca-Ornelas, L.; Patel, D.S.; Bartels, T. Refolding of Helical Soluble α-Synuclein through Transient Interaction with Lipid Interfaces. *FEBS Lett.* **2018**, *592*, 1464–1472. [CrossRef]
100. Wang, C.K.; Wacklin, H.P.; Craik, D.J. Cyclotides Insert into Lipid Bilayers to Form Membrane Pores and Destabilize the Membrane through Hydrophobic and Phosphoethanolamine-Specific Interactions. *J. Biol. Chem.* **2012**, *287*, 43884–43898. [CrossRef] [PubMed]
101. Carneiro, F.A.; Lapido-Loureiro, P.A.; Cordo, S.M.; Stauffer, F.; Weissmüller, G.; Bianconi, M.L.; Juliano, M.A.; Juliano, L.; Bisch, P.M.; Da Poian, A.T. Probing the Interaction between Vesicular Stomatitis Virus and Phosphatidylserine. *Eur. Biophys. J.* **2006**, *35*, 145–154. [CrossRef]
102. Andrushchenko, V.V.; Aarabi, M.H.; Nguyen, L.T.; Prenner, E.J.; Vogel, H.J. Thermodynamics of the Interactions of Tryptophan-Rich Cathelicidin Antimicrobial Peptides with Model and Natural Membranes. *Biochim. Biophys. Acta* **2008**, *1778*, 1004–1014. [CrossRef] [PubMed]
103. Dehsorkhi, A.; Castelletto, V.; Hamley, I.W.; Seitsonen, J.; Ruokolainen, J. Interaction between a Cationic Surfactant-like Peptide and Lipid Vesicles and Its Relationship to Antimicrobial Activity. *Langmuir* **2013**, *29*, 14246–14253. [CrossRef]
104. Sauder, R.; Seelig, J.; Ziegler, A. Thermodynamics of Lipid Interactions with Cell-Penetrating Peptides. In *Cell-Penetrating Peptides: Methods and Protocols, Methods in Molecular Biology*; Langel, Ü., Ed.; Springer Science+Business Media: New York, NY, USA, 2011; Volume 683, pp. 129–155, ISBN 9781607619192.
105. Kerek, E.; Hassanin, M.; Zhang, W.; Prenner, E.J. Preferential Binding of Inorganic Mercury to Specific Lipid Classes and Its Competition with Cadmium. *Biochim. Biophys. Acta Biomembr.* **2017**, *1859*, 1211–1221. [CrossRef] [PubMed]
106. Klasczyk, B.; Knecht, V.; Lipowsky, R.; Dimova, R. Interactions of Alkali Metal Chlorides with Phosphatidylcholine Vesicles. *Langmuir* **2010**, *26*, 18951–18958. [CrossRef]

107. Krylova, O.O.; Jahnke, N.; Keller, S. Membrane Solubilisation and Reconstitution by Octylglucoside: Comparison of Synthetic Lipid and Natural Lipid Extract by Isothermal Titration Calorimetry. *Biophys. Chem.* **2010**, *150*, 105–111. [CrossRef]
108. Pruchnik, H.; Bonarska-Kujawa, D.; Żyłka, R.; Oszmiański, J.; Kleszczyńska, H. Application of the DSC and Spectroscopy Methods in the Analysis of the Protective Effect of Extracts from the Blueberry Fruit of the Genus Vaccinium in Relation to the Lipid Membrane. *J. Therm. Anal. Calorim.* **2018**, *134*, 679–689. [CrossRef]
109. Huh, N.-W.W.; Porter, N.A.A.; McIntosh, T.J.J.; Simon, S.A.A. The Interaction of Polyphenols with Bilayers: Conditions for Increasing Bilayer Adhesion. *Biophys. J.* **1996**, *71*, 3261–3277. [CrossRef] [PubMed]
110. Caturla, N.; Pérez-Fons, L.; Estepa, A.; Micol, V. Differential Effects of Oleuropein, a Biophenol from *Olea europaea*, on Anionic and Zwiterionic Phospholipid Model Membranes. *Chem. Phys. Lipids* **2005**, *137*, 2–17. [CrossRef] [PubMed]
111. Ulrih, N.P.; Maričić, M.; Ota, A.; Šentjurc, M.; Abram, V. Kaempferol and Quercetin Interactions with Model Lipid Membranes. *Food Res. Int.* **2015**, *71*, 146–154. [CrossRef]
112. Selvaraj, S.; Krishnaswamy, S.; Devashya, V.; Sethuraman, S.; Krishnan, U.M. Influence of Membrane Lipid Composition on Flavonoid-Membrane Interactions: Implications on Their Biological Activity. *Prog. Lipid Res.* **2015**, *58*, 1–13. [CrossRef]
113. Malekar, S.A.; Sarode, A.L.; Bach, A.C.; Worthen, D.R. The Localization of Phenolic Compounds in Liposomal Bilayers and Their Effects on Surface Characteristics and Colloidal Stability. *AAPS PharmSciTech* **2016**, *17*, 1468–1476. [CrossRef] [PubMed]
114. Altunayar-Unsalan, C.; Unsalan, O.; Mavromoustakos, T. Insights into Molecular Mechanism of Action of Citrus Flavonoids Hesperidin and Naringin on Lipid Bilayers Using Spectroscopic, Calorimetric, Microscopic and Theoretical Studies. *J. Mol. Liq.* **2022**, *347*, 118411. [CrossRef]
115. Coones, R.T.; Karonen, M.; Green, R.J.; Frazier, R. Interactions of Galloylated Polyphenols with a Simple Gram-Negative Bacterial Membrane Lipid Model. *Membranes* **2024**, *14*, 47. [CrossRef] [PubMed]
116. Chiu, M.; Prenner, E. Differential Scanning Calorimetry: An Invaluable Tool for a Detailed Thermodynamic Characterization of Macromolecules and Their Interactions. *J. Pharm. Bioallied Sci.* **2011**, *3*, 39–59. [CrossRef] [PubMed]
117. Jelesarov, I.; Bosshard, H.R. Isothermal Titration Calorimetry and Differential Scanning Calorimetry as Complementary Tools to Investigate the Energetics of Biomolecular Recognition. *J. Mol. Recognit.* **1999**, *12*, 3–18. [CrossRef]
118. Huang, C. Structural Organization and Properties of Membrane Lipids. In *Cell Physiology Source Book*; Sperelakis, N., Ed.; Academic Press: San Diego, CA, USA, 2001; pp. 43–63.
119. Šturm, L.; Ulrih, N.P. Basic Methods for Preparation of Liposomes and Studying Their Interactions with Different Compounds, with the Emphasis on Polyphenols. *Int. J. Mol. Sci.* **2021**, *22*, 6547. [CrossRef]
120. Patil, Y.P.; Jadhav, S. Novel Methods for Liposome Preparation. *Chem. Phys. Lipids* **2014**, *177*, 8–18. [CrossRef] [PubMed]
121. Vitkova, V.; Hazarosova, R.; Valkova, I.; Momchilova, A.; Staneva, G. Glycerophospholipid Polyunsaturation Modulates Resveratrol Action on Biomimetic Membranes. *Colloids Surf. B Biointerfaces* **2024**, *238*, 113922. [CrossRef] [PubMed]
122. Li, X.; Jiang, H.; Pu, Y.; Cao, J.; Jiang, W. Inhibitory Effect of Condensed Tannins from Banana Pulp on Cholesterol Esterase and Mechanisms of Interaction. *J. Agric. Food Chem.* **2019**, *67*, 14066–14073. [CrossRef]
123. Manach, C.; Scalbert, A.; Morand, C.; Rémésy, C.; Jiménez, L. Polyphenols: Food Sources and Bioavailability. *Am. J. Clin. Nutr.* **2004**, *79*, 727–747. [CrossRef] [PubMed]
124. Jakobek, L. Interactions of Polyphenols with Carbohydrates, Lipids and Proteins. *Food Chem.* **2015**, *175*, 556–567. [CrossRef]
125. Pripp, A.H.; Vreeker, R.; van Duynhoven, J. Binding of Olive Oil Phenolics to Food Proteins. *J. Sci. Food Agric.* **2005**, *85*, 354–362. [CrossRef]
126. Lombardi, L.; Stellato, M.I.; Oliva, R.; Falanga, A.; Galdiero, M.; Petraccone, L.; D'Errico, G.; De Santis, A.; Galdiero, S.; Del Vecchio, P. Antimicrobial Peptides at Work: Interaction of Myxinidin and Its Mutant WMR with Lipid Bilayers Mimicking the *P. aeruginosa* and *E. coli* Membranes. *Sci. Rep.* **2017**, *7*, srep44425. [CrossRef]
127. Sikorska, E.; Dawgul, M.; Greber, K.; Iłowska, E.; Pogorzelska, A.; Kamysz, W. Self-Assembly and Interactions of Short Antimicrobial Cationic Lipopeptides with Membrane Lipids: ITC, FTIR and Molecular Dynamics Studies. *Biochim. Biophys. Acta* **2014**, *1838*, 2625–2634. [CrossRef] [PubMed]
128. Santos-Buelga, C.; Scalbert, A. Proanthocyanidins and Tannin-like Compounds—Nature, Occurrence, Dietary Intake and Effects on Nutrition and Health. *J. Sci. Food Agric.* **2000**, *80*, 1094–1117. [CrossRef]
129. Obreque-Slier, E.; Peña-Neira, Á.; López-Solís, R. Interactions of Enological Tannins with the Protein Fraction of Saliva and Astringency Perception Are Affected by PH. *LWT-Food Sci. Technol.* **2012**, *45*, 88–93. [CrossRef]
130. Shpigelman, A.; Israeli, G.; Livney, Y.D. Thermally-Induced Protein-Polyphenol Co-Assemblies: Beta Lactoglobulin-Based Nanocomplexes as Protective Nanovehicles for EGCG. *Food Hydrocoll.* **2010**, *24*, 735–743. [CrossRef]
131. Stojadinovic, M.; Radosavljevic, J.; Ognjenovic, J.; Vesic, J.; Prodic, I.; Stanic-Vucinic, D.; Cirkovic Velickovic, T. Binding Affinity between Dietary Polyphenols and β-Lactoglobulin Negatively Correlates with the Protein Susceptibility to Digestion and Total Antioxidant Activity of Complexes Formed. *Food Chem.* **2013**, *136*, 1263–1271. [CrossRef]
132. Gonçalves, R.; Mateus, N.; De Freitas, V. Influence of Carbohydrates on the Interaction of Procyanidin B3 with Trypsin. *J. Agric. Food Chem.* **2011**, *59*, 11794–11802. [CrossRef]

133. Jung, M.H.; Seong, P.N.; Kim, M.H.; Myong, N.H.; Chang, M.J. Effect of Green Tea Extract Microencapsulation on Hypertriglyceridemia and Cardiovascular Tissues in High Fructose-Fed Rats. *Nutr. Res. Pract.* **2013**, *7*, 366–372. [CrossRef]
134. Ozawa, T.; Lilley, H. Terence; Haslam Edwin Polyphenol Interactions: Astrigency and the Loss of Astrigency in Ripening Fruit. *Phytochemistry* **1987**, *26*, 2937–2942. [CrossRef]
135. Taira, S.; Ono, M.; Matsumoto, N. Reduction of Persimmon Astringency by Complex Formation between Pectin and Tannins. *Postharvest Biol. Technol.* **1997**, *12*, 265–271. [CrossRef]
136. Houtman, J.C.D.; Brown, P.H.; Bowden, B.; Yamaguchi, H.; Appella, E.; Samelson, L.E.; Schuck, P. Studying Multisite Binary and Ternary Protein Interactions by Global Analysis of Isothermal Titration Calorimetry Data in SEDPHAT: Application to Adaptor Protein Complexes in Cell Signaling. *Protein Sci.* **2007**, *16*, 30–42. [CrossRef]
137. Cotrina, E.Y.; Gimeno, A.; Llop, J.; Jiménez-Barbero, J.; Quintana, J.; Valencia, G.; Cardoso, I.; Prohens, R.; Arsequell, G. Calorimetric Studies of Binary and Ternary Molecular Interactions between Transthyretin, Aβ Peptides, and Small-Molecule Chaperones toward an Alternative Strategy for Alzheimer's Disease Drug Discovery. *J. Med. Chem.* **2020**, *63*, 3205–3214. [CrossRef] [PubMed]
138. Chang, J.W.; Armaou, A.; Rioux, R.M. Continuous Injection Isothermal Titration Calorimetry for in Situ Evaluation of Thermodynamic Binding Properties of Ligand-Receptor Binding Models. *J. Phys. Chem. B* **2021**, *125*, 8075–8087. [CrossRef] [PubMed]
139. Chang, J.W.; Mu, Y.; Armaou, A.; Rioux, R.M. Direct Determination of High-Affinity Binding Constants by Continuous Injection Isothermal Titration Calorimetry. *J. Phys. Chem. B* **2023**, *127*, 10833–10842. [CrossRef]
140. Johannes Gutenberg University Mainz, I. of P. and B.S. ITC-Calculator. Available online: https://www.pharmazie.uni-mainz.de/ (accessed on 10 December 2024).
141. Zheng, F.; Jiang, X.; Wen, Y.; Yang, Y.; Li, M. Systematic Investigation of Machine Learning on Limited Data: A Study on Predicting Protein-Protein Binding Strength. *Comput. Struct. Biotechnol. J.* **2024**, *23*, 460–472. [CrossRef] [PubMed]
142. Li, Z.; Huang, R.; Xia, M.; Patterson, T.A.; Hong, H. Fingerprinting Interactions between Proteins and Ligands for Facilitating Machine Learning in Drug Discovery. *Biomolecules* **2024**, *14*, 72. [CrossRef]
143. Wang, D.D.; Ou-Yang, L.; Xie, H.; Zhu, M.; Yan, H. Predicting the Impacts of Mutations on Protein-Ligand Binding Affinity Based on Molecular Dynamics Simulations and Machine Learning Methods. *Comput. Struct. Biotechnol. J.* **2020**, *18*, 439–454. [CrossRef] [PubMed]